

UC Davis

UC Davis Previously Published Works

Title

Carbides and Nitrides of Zirconium and Hafnium.

Permalink

<https://escholarship.org/uc/item/4vz5357b>

Journal

Materials (Basel, Switzerland), 12(17)

ISSN

1996-1944

Authors

Ushakov, Sergey V
Navrotsky, Alexandra
Hong, Qi-Jun
[et al.](#)

Publication Date

2019-08-01




DOI

10.3390/ma12172728

Peer reviewed

Review

Carbides and Nitrides of Zirconium and Hafnium

Sergey V. Ushakov ^{1,*} , Alexandra Navrotsky ^{1,*} , Qi-Jun Hong ^{2,*} and Axel van de Walle ^{2,*} 

¹ Peter A. Rock Thermochemistry Laboratory and NEAT ORU, University of California at Davis, Davis, CA 95616, USA

² School of Engineering, Brown University, Providence, RI 02912, USA

* Correspondence: svushakov@ucdavis.edu (S.V.U.); anavrotsky@ucdavis.edu (A.N.); qhong@alumni.caltech.edu (Q.-J.H.); avdw@brown.edu (A.v.d.W.)

Received: 6 August 2019; Accepted: 22 August 2019; Published: 26 August 2019



Abstract: Among transition metal carbides and nitrides, zirconium, and hafnium compounds are the most stable and have the highest melting temperatures. Here we review published data on phases and phase equilibria in Hf-Zr-C-N-O system, from experiment and ab initio computations with focus on rocksalt Zr and Hf carbides and nitrides, their solid solutions and oxygen solubility limits. The systematic experimental studies on phase equilibria and thermodynamics were performed mainly 40–60 years ago, mostly for binary systems of Zr and Hf with C and N. Since then, synthesis of several oxynitrides was reported in the fluorite-derivative type of structures, of orthorhombic and cubic higher nitrides Zr_3N_4 and Hf_3N_4 . An ever-increasing stream of data is provided by ab initio computations, and one of the testable predictions is that the rocksalt $HfC_{0.75}N_{0.22}$ phase would have the highest known melting temperature. Experimental data on melting temperatures of hafnium carbonitrides are absent, but minimum in heat capacity and maximum in hardness were reported for Hf(C,N) solid solutions. New methods, such as electrical pulse heating and laser melting, can fill the gaps in experimental data and validate ab initio predictions.

Keywords: zirconium carbide; hafnium carbide; zirconium nitride; hafnium nitride

1. Introduction

The carbides and nitrides of zirconium and hafnium provide a reservoir of very effective refractory materials, including some compounds that have been predicted to have the highest melting points [1]. Ti, Zr, and Hf belong to group IVb of transition metals. These so-called titanium group elements form the most stable nitrides and carbides known [2]. They share NaCl-type (rocksalt) structure, high thermal and electrical conductivity, strength, and hardness. Titanium carbide and carbonitrides have been used as cermets constituents since 1970; most of the produced tools for metal cutting are coated with multilayer TiN-TiCN-TiC coatings, applied through physical or chemical vapor deposition processes. These coatings reduce wear through increased hardness and lowering frictional welding at high operating speed [3]. For the last three decades, more than 1000 papers have been published every year on Ti carbides and nitrides (Figure 1). Although melting temperatures for carbides and nitrides of zirconium and hafnium are higher than those for Ti, they are studied less and their applications are currently limited.

There are more publications on ZrC per year than for ZrN, HfC, and HfN combined. This is driven by the research on ZrC for nuclear-related applications such as barrier coatings for nuclear rocket reactors [4] and replacement of SiC in tri-isotropic (TRISO) fuel for high temperature nuclear reactors [5]. Nitrides of actinides are studied as advanced nuclear fuels compatible with liquid metal coolant, and ZrN is a primary matrix candidate for Pu based nuclear fuel [6].

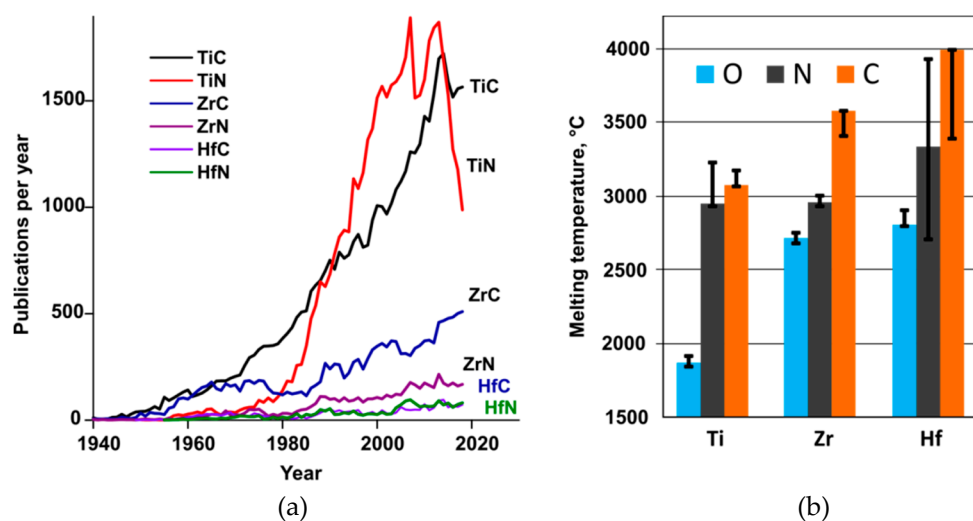


Figure 1. (a) Number of publications per year on carbides and nitrides of titanium group transitional metals (1940–2018 Chemical Abstract database). (b) The preferred values for melting temperatures of Ti, Zr, and Hf carbides and nitrides with NaCl-type structure. See Section 4 for references. The “error bars” indicate the range of previously reported values for melting temperatures from Berg et al. [7].

Due to high neutron absorption of Hf, its carbides and nitrides did not receive as much attention as zirconium counterparts for nuclear-related applications; however, they have a high potential for advanced solar energy-related applications. Partially oxidized hafnium carbide coatings showed high spectral selectivity as absorber coating for concentrated solar power systems [8], and hafnium nitride as an absorber for hot carrier solar cells [9]. For polymer electrolyte membrane fuel cells, ZrN coating was shown to significantly increase corrosion resistance and hydrophobicity of stainless steel for replacement of highly brittle graphite-based bipolar plates [10].

Zirconium and hafnium nitrides are also attractive hard coatings for decorative and architectural glass applications [11]. They have golden-green and yellow-green colors, which can be fine-tuned by nitride stoichiometry and by alloying with Ti and Al nitrides and carbides [12]. Zirconium nitride coated tools and scalpel blades are commercially available and are considered to be superior for Al cutting applications and have high biocompatibility.

Recently, Zr and Hf oxynitrides made it into the playbook of the semiconductor industry since current leakage through thermally grown SiO₂ thin films forced a search for a suitable replacement material with a higher dielectric constant. Amorphous Zr and Hf oxynitrides are researched as gate dielectrics in integrated circuits [13–16]. Hafnium oxynitride also forms on SiN–HfO₂ interface, where HfO₂ used as gate dielectric and SiN as a diffusion barrier on Si [17].

Finally, one should mention the application which funded most of the research on refractory carbides, nitrides, and borides at high temperature: it is their use as constituents of ultra high temperature ceramics, studied since the 1950s for thermal protection systems for atmospheric reentry and, more recently, for sharp leading edges of hypersonic missiles [18,19].

Carbides and nitrides of Zr and Hf were previously reviewed together with other transition metals in monographs by Goldschmidt [20] and Storms in 1967 [21], Toth in 1971 [22], Pierson in 1996 [23], and in a collection of papers edited by Freer in 1990 [24], Samsonov in 1995 [25], Oyama in 1996 [26], Gogotsi and Andrievski in 1999 [27]. Catalytic properties were reviewed by Levy in 1977 [28] and by Ham and Lee in 2009 [29]. Monograph by Turchanins 1991 [30] presented in details 20-year of original experimental work on the thermodynamics of refractory carbides and carbonitrides, some of which were previously published in English [31–34], but the monograph is only available in Russian. Samsonov, Upadhyaya, and Neshpor published in Russian a monograph on carbides in 1974 [35]. The updated and extended monograph was published by Upadhyaya 1996 [36] in English. This encyclopedic, 500 pages compendium also covers binary and ternary systems with boron and nitrogen

and based on more than 2000 original research reports published before 1980. During the last 20 years, Lengauer et al. [37–41] provided comprehensive reviews and new experimental data on solid state properties of Ti group carbonitrides. Finally, the second volume of Shabalin's (2019) [42] monograph on ultra-high temperature materials provides an exhaustive 350 pages reference on chemical and physical properties of hafnium and zirconium monocarbides.

In this paper, we review thermodynamic data available from experiment and computations for the Zr-C-N and Hf-C-N systems. Our focus is on rocksalt (δ -phase) (oxy)carbonitrides: monocarbide and mononitrides of Zr and Hf, their solid solutions, and oxygen solubility limits. They are the only compounds in these systems that melt without decomposition and are traditionally considered most interesting for applications. We will briefly touch on non-metallic higher nitrides: Zr_3N_4 and Hf_3N_4 attracted a lot of attention due to the change from insulator to metallic conductivity upon nitrogen loss [43–47] and their hardness in Th_3P_4 -type structure, stable at high pressure, but also synthesized as coatings at ambient pressure.

First, we briefly overview synthesis methods, established binary phase diagrams, and reported and predicted phases. Then, we review the structure and thermochemistry of rocksalt (oxy)carbonitrides and list recommendations for future experimental and computational works.

2. Synthesis Methods

Zirconium and hafnium carbides and nitrides can be synthesized by direct reaction of metal or metal hydride powders with graphite or N_2 . The reactions are strongly exothermic and can be used in a self-propagated high temperature synthesis (SHS) process [48]. The reaction of oxides with graphite (carbothermal process) is widely used for industrial synthesis of bulk carbide powders. Nitrides can also be synthesized from oxides [49] by reaction with nitrogen or ammonia, usually in the presence of carbon (carbothermal nitridation) [26,50]. The traditional preparation routes were reviewed in monographs by Toth [22] and Storms [21]. The enthalpies and entropies for the selected reactions are presented in Table S1.

Recent research efforts in the synthesis of carbides and oxycarbides were aimed at the production of fine powders. For ZrC , this was achieved using polymer precursors or zirconia sol-sucrose mixture, or by decomposition of zirconium-based metal-organic frameworks (MOFs) [51]. ZrN powders with submicron size were also recently synthesized by reduction of ZrO_2 with Al metal in N_2 atmosphere [52] using CaCO_3 addition to form HCl-soluble calcium aluminate and zirconate phases. This method was inspired by a similar route earlier employed for TiN [53], and many syntheses approaches established for TiN and TiC can be adapted for Zr and Hf carbides and nitrides.

The variety of chemical and physical vapor deposition (CVD and PVD, respectively) methods for refractory carbides was reviewed by Pierson (1996) [23], although more research was focused on titanium carbonitrides. Carbides, nitrides, and carbonitrides of Zr and Hf can be prepared by CVD at 900–1200 °C from metal chlorides (ZrCl_4 or HfCl_4) and nitrogen or ammonia as a source of nitrogen or hydrocarbons as a carbon source. These CVD reactions usually proceed in the presence of hydrogen. HfC deposition by CVD was demonstrated using methane (CH_4), propane (C_3H_8), propene (C_3H_6), or toluene (C_7H_8) and methyl chloride (CH_3Cl). Apart from TiCl_4 , hafnium, and zirconium, chlorides are solid at room temperature, but can be synthesized in situ by metal reaction with Cl or HCl at 500–600 °C. Carbide and nitride coatings can also be produced by PVD methods, e.g., reactive evaporation of metals in nitrogen, ammonia or hydrocarbon atmospheres, molecular beam evaporation, sputtering, and ion plating [54].

Zr and Hf carbides and nitrides form continuous solid solutions in the rocksalt structure and can contain substantial amounts of oxygen. This makes it possible to obtain different compositions and tune the properties by slight adjustments of synthesis conditions; however, it also makes it challenging to reproducibly synthesize pure compounds with well-defined stoichiometry. Carbides obtained by carbothermal reaction from oxides are known to retain some oxygen [55]. Nitrides from carbothermal nitridation will contain both oxygen and carbon impurities [50]. Synthesis from metal

hydrides is often considered most appropriate for producing pure compounds; however, hydrogen can also be incorporated in rock-salt structure, e.g., formation of the solid solution $\text{ZrC}_{0.67}\text{H}_{0.33}$ has been reported [56]. The continuous solid solutions, coupled with nonstoichiometry and technical difficulties analyzing light elements, are the reasons for large scatter in structural data and properties attributed to nominally same compositions from different synthesis routes as discussed below.

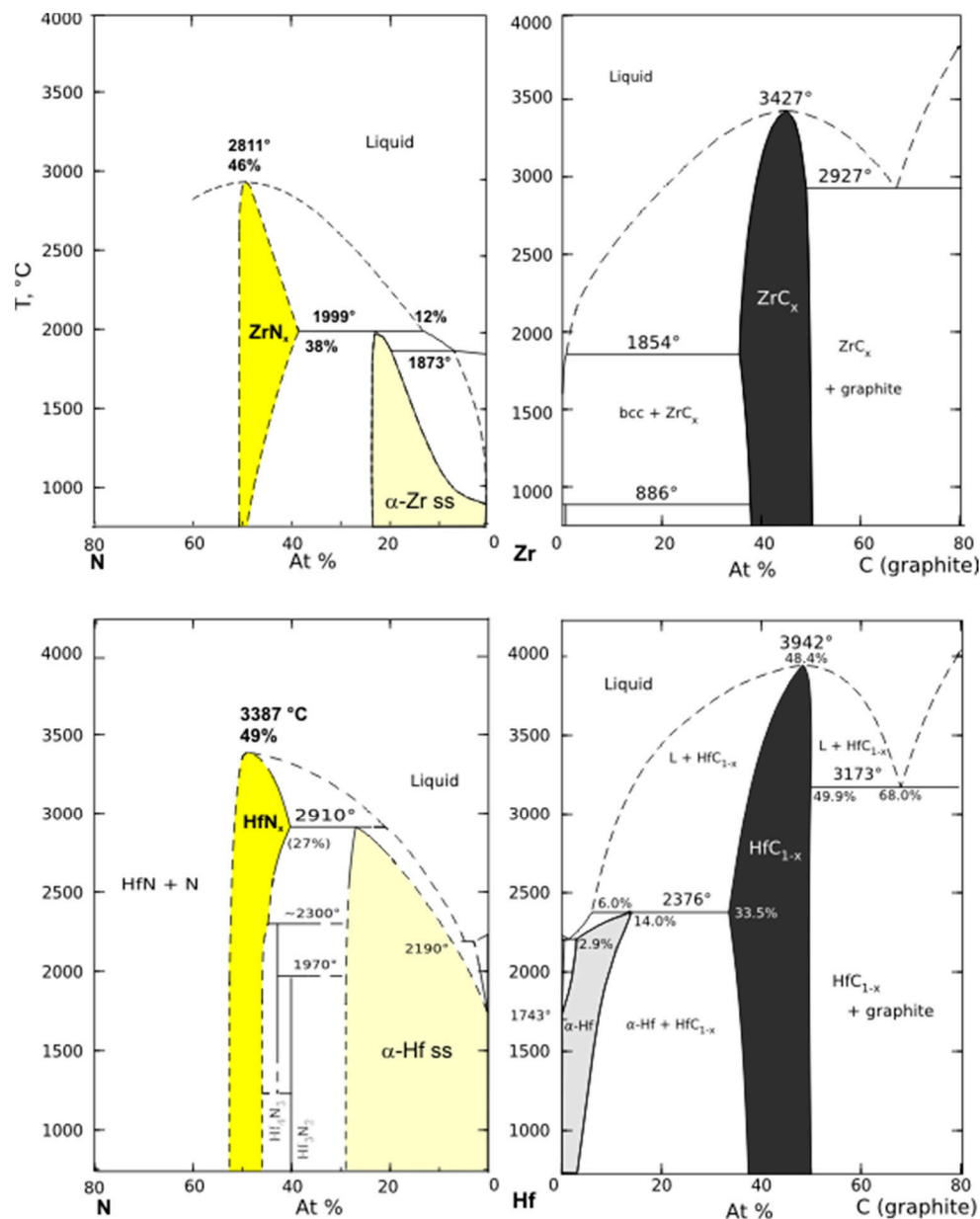


Figure 2. Binary phase diagrams for condensed system of Zr and Hf with graphite and nitrogen (at 1 atm pressure), redrawn after: (Zr-N)—Ma et al. (2004) [57]; (Zr-C)—Gullerment (1995) [58]; (Hf-N)—Okamoto (1990) [59]; (Hf-C)—Bittermann and Rogl (1997) [60].

3. Phase Diagrams

The binary systems of zirconium and hafnium with nitrogen and carbon were studied experimentally from circa 1000 °C to liquidus temperatures and most of the systematic studies of phase equilibria were performed before 1970. New experimental results on melting temperature determination and thermodynamic properties of single phases were published since then [61–66], and an entirely new stream of thermodynamic data has emerged from ab initio computations [1,67–69].

The state of the art calculation of phase diagrams (Calphad) method [70–73] allows for the calculation of phase equilibria in multicomponent systems above room temperature at atmospheric pressure, providing that Gibbs free energy functions for all phases from room temperature to the melting point and above can be derived from observed phase equilibria and thermodynamic data. In Calphad assessments, ab initio computational results are treated on the same footing as experimental data.

The availability and accuracy of experimental data for metals [74,75] and a unified set of unary data [76] have enabled the great practical success of the Calphad approach for the engineering of metal alloys [77,78]. Calphad application to carbides, nitrides, and oxides is hampered by lack of data and complexity of structures. The latest binary phase diagrams for Hf and Zr systems with nitrogen and carbon are shown in Figure 2. Thermodynamic assessment using the Calphad method was performed on Zr-C, Hf-C, and Zr-N systems by Guillermet in 1995 [58], Bittermann and Rogl in 1997 [60] and Ma et al. in 2004 [57], respectively. No Calphad assessment of Hf-N system is available.

3.1. Zr-C, Hf-C, and Zr-Hf-C

Calphad assessment of Zr-C system by Guillermet [58] relied on phase equilibria data from Sara [79] and Rudy [80], selected values for enthalpies of formation and high temperature heat contents for $\text{ZrC}_{0.69}$ – $\text{ZrC}_{0.99}$, and low-temperature heat capacity and entropy for $\text{ZrC}_{0.96}$. Guillermet [58] found significant discrepancies between different reports on high temperature heat capacities of Zr carbides and did not use them in his optimization. Since then, a review on ZrC properties was published by Jackson and Lee [81], which provides a comprehensive compilation of thermodynamic data on ZrC system including heat capacities as a function of C/Zr ratio. Guillermet's [58] assessment of the Zr-C system was used in a number of later Calphad assessments of ternary systems [55,82].

Calphad treatment of Hf-C system by Bittermann and Rogl [60] follows the version of the experimental phase diagram presented by Rudy (1969) [80]. Formation enthalpy and high temperature heat content for HfC_{1-x} was included in the optimization. The calculated phase diagram reproduces well most of Rudy's [80] experimental points, with the exception of liquidus boundaries on Hf-HfC side. Bittermann and Rogl [60] attribute this difference to inherent uncertainties in the Pirani method [83] used by Rudy to obtain liquidus data. In a 2001 review of Hf-C system by Okamoto [84], Bittermann and Rogl's [60] assessment is accepted as a better representation of the system than original work by Rudy [80].

Bitterman and Rogl [85] also performed a thermodynamic assessment of the Zr-Hf-C ternary system. It was based almost exclusively on an extensive 1966 study of phase equilibria [86]. ZrC and HfC form continuous solid solutions with lattice parameter decreasing close to linear from 4.7 to 4.63 for $(\text{Zr,Hf})\text{C}_{0.75}$ and linear increase in melting point from 3430 °C $\text{ZrC}_{0.8}$ to 3830 °C for $\text{HfC}_{0.98}$. Upadhayaya's cited three sources in Russian from the 1960s, two of which reported a maximum in melting point, and one did not. Complete miscibility between rocksalt HfC and ZrC down to 185 K was predicted from ab initio study using cluster expansion approach [87].

Subcarbides

Obata and Nakazawa [88] observed superlattice formation in $\text{ZrC}_{0.7}$ ($\text{Zr}_4\text{C}_{3-x}$) from X-ray diffraction, resulting in a lattice parameter (9.386 Å) twice of that of rocksalt ZrC. They reported order-disorder transformation to defective rocksalt structure at ~1100 °C. Hu et al. [89] observed domains with Zr_2C type ordering in $\text{ZrC}_{0.61}$ sample prepared by spark plasma sintering (SPS). However, no structures were refined by either author. No Hf subcarbides were reported.

Weinberger and Thompson [68] performed computations on the Zr-C and Hf-C systems using density functional theory and the order-parameter functional method. For the Zr-C system below 1000 °C, they predicted a number of vacancy-ordered structures (Zr_2C , Zr_3C_2 , Zr_6C_5), which transform to sodium chloride type ZrC_{1-x} at a higher temperature. Their computations indicated that Zr_4C_3 phase is unstable, although it is close to $\text{ZrC}_{0.7}$ composition in which superlattice reflections were

experimentally reported [88]. Subcarbides were not included in the latest Calphad optimizations of the systems.

3.2. Zr-N and Hf-N

A Calphad optimization of Zr-N system was performed by Ma et al. [24] using experimental data from Domagala et al. [90] for Zr-rich part and enthalpies of formation estimated from ab initio computations. The diagram was reassessed by Sridar et al. [91] as part of the modeling of the Ti-Zr-N system using additional thermodynamic data, such as the formation enthalpy of ZrN_{1-x} [92].

The Hf-N system was presented by Okamoto in 1990 [59] from reported experimental data on phase equilibria. No Calphad optimization was performed on a system. We located only one measurement of formation enthalpy of hafnium nitride, which was performed by Humphrey in 1953 [93]. Its reliability is discussed below in a section on rocksalt carbonitrides.

3.2.1. Subnitrides

Subnitrides Hf_3N_2 and Hf_4N_3 were first prepared by Rudy in 1970 [94] by the reaction of Hf metal with HfN and reported to be stable below 1970 and 2300 °C, respectively. Both compounds have a trigonal structure which can be described as stacking of Hf layers with hexagonal close packing of α -Hf and cubic close packing as in HfN. Rudy [94] refined the structure from powder X-ray diffraction but could not determine if nitrogen atoms are randomly distributed in octahedral interstices or ordered. Lengauer et al. [95] prepared both hafnium subnitride compounds as single phases via diffusion couples and suggested to name them as *eta* (η - $\text{Hf}_3\text{N}_{2-x}$) and *zeta* (ζ - $\text{Hf}_4\text{N}_{3-x}$) phases to be consistent with known isostructural nitrides and carbides of transitional metal. *Eta* subnitride is observed in the Ti-N system as well. *Zeta* subcarbide phase is known in the Ta-C system and is associated with high fracture toughness. The computational investigation of microstructure and stability of ζ - $\text{Hf}_4\text{N}_{3-x}$ together with isostructural Nb and V subcarbides was undertaken by Weinberger et al. (2018) [69]. They concluded that stoichiometric *eta* and *zeta* phases are thermodynamically stable in the Hf-N system, but metastable in carbides. No subnitride phases have been reported for the Zr-N system.

3.2.2. Higher Nitrides

In a 1990 review of the Hf-N system, Okamoto stated succinctly that “no information is available on the N-rich side of the diagram” [59]. Ma et al. [57] computed enthalpy of formation for hypothetical ZrN_3 to be used in Calphad optimizations of the Zr-N system, but no nitrides with N/Me ratio >1 are shown on the final diagram, assessed from 500 to 5500 K. Yet, higher nitrides of Zr and Hf and Ti do exist and are the subject of intense theoretical [96–104] and experimental [44,46,97,105–107] investigations.

Zr_3N_4 was first synthesized in the 1960s by the reaction of ZrI_4 [43] and ZrCl_4 [108] and was shown to be an insulator and to decompose to ZrN and N_2 above 1100 °C. Twenty years later, it was rediscovered by Schwartz et al. [46] at the IBM research center, who obtained transparent films while varying the N/Zr ratio in the dual ion-beam sputtering process. It took 10 more years before Lerch et al. [44] refined the Zr_3N_4 crystal structure from powder sample as orthorhombic (*Pnma*). The isostructural Hf_3N_4 was not reported. The hardness of orthorhombic Zr_3N_4 is similar to that of rocksalt ZrN. The transition from transparent insulator to metallic coating is of independent interest for potential applications.

In 2003, the synthesis of cubic Zr and Hf higher nitrides with Th_3P_4 (*I-43d*) structure was reported in laser-heated diamond cell experiments at 18 GPa at ~2500 °C [45] and, two years later, Zr_3N_4 was synthesized in this phase at atmospheric pressure by reactive evaporation technique [109]. The hardness of the c- Zr_3N_4 coating exceeds those of ZrN and TiN.

Recent ab initio computations showed that orthorhombic (*Pnma*) Hf_3N_4 is stable at ambient pressure [110,111]. However, Zhang et al. [103] found using first principles evolutionary calculations that *Pnma*- Hf_3N_4 is stable at 2–9 GPa range (while a Zr_3N_4 analog was synthesized [44] at ambient

pressure) but predicted that triclinic and monoclinic higher nitrides $\text{Hf}_{11}\text{N}_{12}$, Hf_7N_8 , and Hf_4N_5 and Hf_3N_4 are stable at zero pressure (Table 1).

Table 1. Phases reported and predicted in Hf-C-N-O and Zr-C-N-O systems at ambient pressure.

Phases	SG	Str. Type	Comments, [Refs]
Reported from the experiments at 1 Atm			
$\delta\text{-Hf}_2\text{Zr(C,N,O)}$	<i>Fm-3m</i>	NaCl (B1)	[38,55,112–114]
$\eta\text{-Hf}_3\text{N}_2$	<i>R-3m</i>	Ta_2VC_2	[94,95]
$\zeta\text{-Hf}_4\text{N}_3$	<i>R-3m</i>	Hf_4N_3	[94,95]
Zr_3N_4	<i>Pnma</i>		[115]
Zr_3N_4	<i>I-43d</i>	Th_3P_4	[109]
$\beta\text{-Zr}_7\text{O}_8\text{N}_4$	<i>R-3H</i>	Pr_7O_{12}	[116]
$\beta'\text{-Zr}_7\text{O}_{11}\text{N}_2$	<i>R-3H</i>	$\text{Zr}_5\text{Sc}_2\text{O}_{13}$	[117]
$\beta''\text{-Zr}_7\text{O}_{9.5}\text{N}_3$			[118]
$\gamma\text{-Zr}_2\text{ON}_2$, Hf_2ON_2	<i>Ia-3</i>	Mn_2O_3	[119]
$\text{Zr}_4\text{O}_5\text{N}_2$	<i>I4cm</i>	Flr-deriv	[120]
Predicted from computations to be stable at 1 atm			
Zr_3C , Hf_3C ,	<i>Pnma</i>	In_3Ir	[121]
Zr_3C_2 Zr_8C_7			[122]
$(\text{Zr,Hf})_2\text{ON}_2$	<i>C1m1</i>	Pv-deriv	[123]
Hf_6N	<i>P-31c</i>		[103]
Hf_2N	<i>Pnnm</i>		[103]
HfN (ZrN)	<i>P63/mmc</i>	TiAs	[103]

3.3. Zr Versus Hf in Binaries with Carbon and Nitrogen

Zirconium and hafnium form rocksalt monocarbides and mononitrides with full mutual solubility, at least above 1000 °C. However, substantial differences are observed between the Zr and Hf systems with carbon and nitrogen.

Zr analogs of *eta* ($\eta\text{-Hf}_3\text{N}_2$) and *zeta* ($\zeta\text{-Hf}_4\text{N}_3$) hafnium subnitrides were not reported (Table 1), neither was synthesis of an Hf analog of Zr_3N_4 at ambient pressure. In metal-rich compositions, hafnium dissolves more carbon and nitrogen than zirconium, which results in stabilization of $\alpha\text{-Hf}$ to higher temperatures. In contrast with Zr, $\beta\text{-Hf}$ is not stable in the presence of HfC . A more detailed study of N positions in $\alpha\text{-Hf}$ may very well uncover different structures in what is now labeled as the $\alpha\text{-Hf(N)}$ solid solution field (Figure 2).

It must be noted that assessments of Zr and Hf binaries with carbon and nitrogen are based on experimental data obtained mostly in the 1960s, and authors are often forced to choose between conflicting datasets. For example, Bitterman and Rogl's (1997) assessment of Hf-C diagram follows the experimental diagram by Rudy (1965). Upadhyaya (1996) favors the diagram by Sara [79], which shows that the $\alpha\text{-Hf}$ phase dissolves up to 18 at.% of C and is stable to 2820 °C. The impurities of O and N in carbide samples used in different studies could shift the observed equilibrium drastically. Thus, we expect that phase relations in the binary systems of Hf and Zr with C and N may undergo substantial revisions and include higher nitrides, subnitrides, and subcarbides as new experimental and computational data become available.

3.4. Zr-C-N, Hf-C-N, Zr-N-O, Hf-N-O Ternaries

The available data on phase equilibria and thermodynamics of ternary systems are scarce and not systematic. Lerch [118] described several ternary compounds in the $\text{ZrO}_2\text{-Zr}_3\text{N}_4$ pseudobinary, which include Zr_2ON_2 (γ -phase with bixbyite structure) and several other fluorite-related structures denoted as β , β' and β'' and listed in Table 1. Above 1000 °C all of them decompose to NaCl-type ZrN and N-stabilized fluorite-type zirconia. Most of the experimental and computational studies were

devoted to rocksalt carbonitrides thermochemistry and properties. These efforts are reviewed in the next section.

4. Rocksalt (oxy)carbonitrides

The rest of the review is focused on structure and thermodynamic properties of (oxy)carbides and (oxy)nitrides of Zr and Hf. Among them, much more data are available for ZrC and were summarized, analyzed, and discussed in an excellent review by Jackson and Lee [81]. The papers by Lengauer et al. [3,38–41,112,124] provide analysis of solid state properties of Zr and Hf compounds in the larger frame of transition metal carbonitrides.

Our aim here is to aid future experimental work, ab initio computations and Calphad optimizations by bringing to light to some relevant data which are often omitted, e.g., formation enthalpies for oxycarbides measured by Kornilov [125], work of Turchanin [30] on compositional dependence of high temperature heat capacity of carbonitrides, and Brundiers [126] work on Hf oxycarbonitrides. We also want to highlight very recent developments, such as the application of the impulse current heating method to measure high-temperature heat capacities and fusion enthalpies for zirconium carbonitrides and ab initio computations of the fusion enthalpies and melting temperatures in the Hf-C-N system.

4.1. Structural Features

Ti, Zr, and Hf carbides and nitrides are found in NaCl-type (rocksalt) structure. Only Ti forms an NaCl-type metallic oxide, with stoichiometry varying from $\text{TiO}_{0.75}$ to $\text{TiO}_{1.3}$ [127]. Besides the alkali halides, the oxides of alkaline earths, many divalent transitional metals (Mn, Fe, Ni) and vanadium monoxide all share a NaCl structure. All rare earth elements (REE) form NaCl-type nitrides, oxycarbides, and carbonitrides but not stoichiometric monocarbides [128]. The monoxides of La, Ce, Nd, Sm, Eu, Y, and Yb with rock salt structures were reported in the 1950s and 1960s [129]. They were synthesized by reduction of sesquioxides with carbon or a corresponding rare earth metal. However, it was later established [130,131] that only divalent YbO and EuO can be synthesized at ambient pressure and earlier reported monoxides of other rare earth elements were, in fact, oxycarbides or oxynitrides (although metallic oxides of trivalent light REE were synthesized in the rocksalt structure at 1.5–8 GPa and 800–1000 °C) [132]. Thorium and uranium also form NaCl-type nitrides and carbides [133], and their potential application as advanced nuclear fuels with high loading is the reason for the keen interest in ZrC as a protective coating and in rare earth carbides as fission products.

The rocksalt structure (Figure 3) can be described as two face-centered cubic lattices of metal and nonmetal moved with respect to each other or as a metal cubic close-packed structure with all octahedral voids occupied by nonmetal. The space group is Fm3m, with coordinates for all atoms defined by space group symmetry: the metal at 0, 0, 0 and the nonmetal at $\frac{1}{2}, \frac{1}{2}, \frac{1}{2}$. Four formula units make up the conventional cubic unit cell ($Z = 4$). The structure can accommodate vacancies on both metal and non-metal sublattices. The carbon-to-metal ratio in Zr and Hf carbides is always less than or equal to 1; thus, their formula is often written as MeC_{1-x} . This formula does not mean that there are no vacancies on the metal sublattice; it only indicates that there are typically fewer vacancies on metal sublattice than on the carbon sublattice. A notable exception is the case of nitrides, since compositions with nitrogen excess, up to $\text{HfN}_{1.2}$ have been reported in the rocksalt structure [126]. The formula could equivalently be written as Hf_{1-x}N , to indicate that the vacancies are predominantly on the metal sublattice.

Figure 4 shows reported lattice cell parameters for Zr and Hf carbides nitrides and their solid solutions. The considerable variation in cell parameters for nominally ZrN composition reported in recent years is likely related to the fact that the thin films samples were produced by CVD and PVD. Due to analytical difficulties in quantifying ratios of C, N, and O in nonstoichiometric carbonitrides, it is tempting to establish lattice parameter composition relations for (oxy)carbonitrides, and many analytical expressions were derived and reported in separate studies [55,81,113,114,134]. However, these parametrizations are likely to be useful only within a set of samples arising from the same

synthesis procedure. Cell parameter for Zr and Hf carbides can be lowered by either carbon deficiency, or by O or N substitution. To complicate things even further, the lattice parameter of ZrC_x as a function of C content shows a maximum at $x = 0.8$, while this is not observed for HfC_x (Figure S1). Hydrogen can also be incorporated in the vacancies of the nonmetal sublattice without a significant effect on the lattice parameter [35]. In this respect, the few reports on the formation enthalpies of these compounds discussed below are valuable references, since in order to derive formation enthalpies from heats of combustion, initial samples, and combustion products were thoroughly characterized, often using a combination of different techniques.

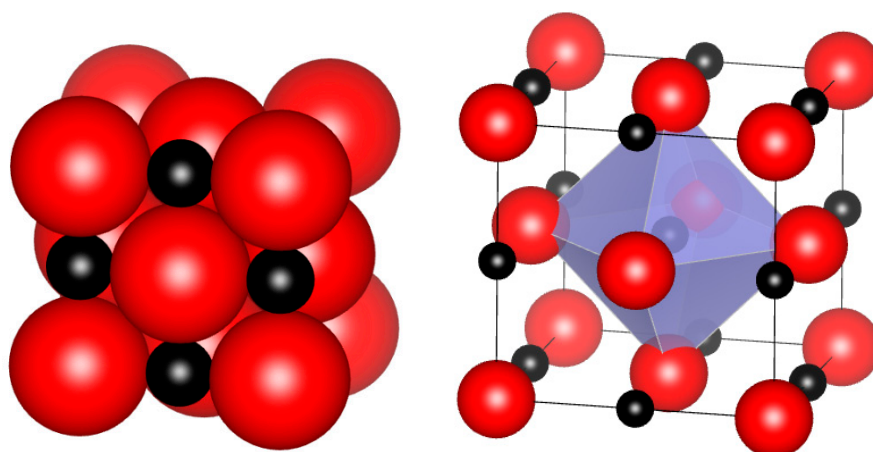


Figure 3. Rocksalt structure in space-filling and polyhedral representations, showing the location of nonmetal atoms in octahedral voids of a face-centered cubic metal sublattice. Red spheres indicate metal atoms.

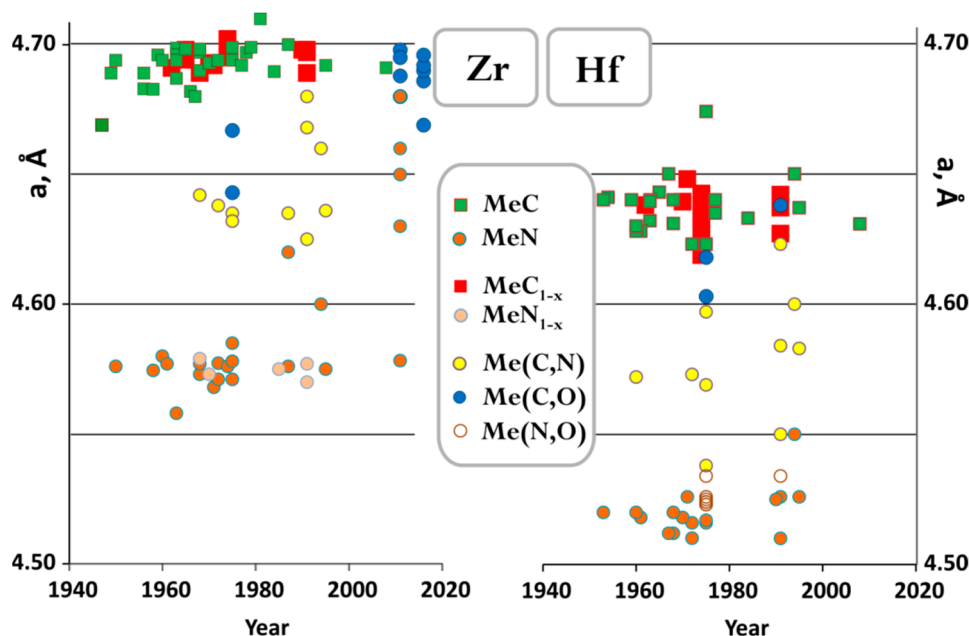


Figure 4. The lattice parameter of NaCl-type compounds. (Left) Hf-C-N-O system. (Right) Zr-C-N-O system. See Table S2 for compositions for each data point.

There are no experimental reports on the high pressure phase transformations of rocksalt-type carbonitrides. Ab initio computations showed that the NaCl structure is stable for ZrC , ZrN , and HfN to at least 150 GPa. The predicted high pressure phase of carbonitride is a CsCl-type structure [67,110], in which coordination increases from 6 to 8 with an associated volume decrease of less than 1.4 %. An

unexpected computational result from Zhang et al. [103] is a prediction that HfN is thermodynamically stable in the rocksalt structure only above 60 GPa or above 400 °C at zero pressure and the ground state of HfN is a hexagonal P63/mmc (TiAs-type) structure, which was never reported in experiments.

4.2. Stability Field of Rocksalt Carbonitrides in Hf-Zr-C-N-O System

Most experimental studies of compositions of rocksalt carbonitrides have been performed on the samples synthesized at 1000–2500 °C. At these temperatures, complete miscibility in the rocksalt structure is observed between ZrN-ZrC and HfN-HfC [112,124] (and presumably in ZrC-ZrN-HfN-HfC). The main questions remaining pertain to the magnitudes of the thermodynamically stable stoichiometry deviations due to deficiencies on either metal or nonmetal sublattices and to oxygen and hydrogen dissolution in the structure.

Binder et al. [112] reported that the maximum deficiency on non-metal sublattice for zirconium carbonitrides at 1150 °C is nearly constant between ZrN_{1-x} and ZrC_{1-x} and is limited to ~60 at% Zr. Brundiers [126] reported isothermal crosssection for Hf-C-N system at 1500 °C showing close to linear Hf-rich boundary from $\text{HfC}_{0.6}$ to $\text{HfN}_{0.7}$. He also studied carbon- and nitrogen-rich compositions and found that deficiency on the Hf sublattice does not occur in solid solutions with more than 20 % HfC (Figure S2).

Constant et al. [114,135] studied oxygen solubility in zirconium and hafnium carbonitrides and their solid solutions. They prepared samples from metallic Zr and Hf mixed with carbides, nitrides, oxides, and carbon. They reported the stability fields in the form of pseudo-ternary crosssections MeO-MeC-MeN (with Me = Zr or Hf). This choice of the end members assumes no deficiency on either the metal or nonmetal sublattices. They found extensive oxygen solubility in zirconium carbonitrides with x in $\text{ZrC}_{1-x}\text{O}_x$ increasing from 0.55 at 1600 °C to 0.75 at 2000 °C, and from 0.35 to 0.55 in $\text{ZrN}_{1-x}\text{O}_x$. They reported that $\text{Hf(N,C)}_{1-x}\text{O}_x$ compositions have lower oxygen solubility limits with maximum values extending from x = 0.2–0.25 at 1600 °C to x = 0.25–0.3 at 2000 °C.

A new investigation of oxygen solubility in ZrC and HfC was published by Rejasse et al. in 2016 [55] and 2017 [113]. They confirmed the higher solubility of oxygen in ZrC relative to HfC but reported much lower limits: x = 0.26 for $\text{ZrC}_{1-x}\text{O}_x$ at 1850 °C and x = 0.10 for $\text{HfC}_{1-x}\text{O}_x$ at 1750 °C. Kornilov et al. [136] performed a characterization of Hf oxycarbides (Table S3) for the purpose of formation enthalpy determination and reported a maximum oxygen content of x = 0.15 in the substoichiometric $\text{HfC}_{0.6}\text{O}_{0.15}$ composition.

Note that in Rejasse's [113] experiments, the samples were synthesized by a carbothermic reduction of oxides with amorphous carbon, which rules out deficiency on the non-metal sublattice. Constant [114,135] and Kornilov [136] both reported higher oxygen dissolution limits in Zr and Hf rocksalt oxycarbides. They used metallic Zr and Hf in the synthesis, thus making metal-rich compositions possible.

The quantitative analysis of oxygen in oxycarbides is experimentally challenging and can be a major source of discrepancies. Rejasse [113] derived free carbon and total carbon from an analysis of CO_2 evolved on combustion in oxygen at 1000 °C and 1800 °C, respectively, and oxygen was analyzed from CO evolved on samples during annealing at 2500–2800 °C in He atmosphere and graphite crucibles. This procedure assumes that above 2500 °C no oxygen is retained in carbonitrides. Kornilov [136] determined oxygen content by both vacuum fusion method and neutron activation analysis and reported that the former substantially underestimate oxygen content, apparently due to irreversible sorption of combustion products. Recently, ion microprobe methods were also applied for oxygen analysis in carbonitrides [137].

4.3. Melting Temperatures of Hafnium Carbides and Carbonitrides

Due to similar chemistry, separating hafnium and zirconium have historically been relatively difficult. The element hafnium was not identified until 1923, making it the last stable element to be discovered. Early studies of the Hf-C system [21,138–142] often involved an impurity of several wt%

of zirconium. Given that ZrC melting temperature is 400 °C lower than HfC (Table 2), this may affect early results in the Hf-C system.

The melting temperature of HfC was first determined as 4160 K (3887 °C) by Agte and Alterthum in 1930 [138]. They also performed melting temperature measurements of binary carbides of Zr, Nb, Mo, Hf, Ta, and W their ternary solid solutions and found that rocksalt compound with composition Ta_4HfC_5 had a melting temperature measured as 4215 K (3942 °C). Although not confirmed by later measurements by Rudy et al. [142], Ta_4HfC_5 had often been considered as the material with the highest known melting point.

The interest in HfC increased significantly in the space age of the 1960s when there was an urgent need for materials with high melting temperatures, high softening temperatures, and other high-temperature properties so that these materials would stand up under extreme temperature conditions, such as in rocket engines or during atmospheric reentry. In 1963, Admas and Beall [140] determined that the highest melting point in the Hf-C system is 3895 °C at $\text{HfC}_{0.985}$. In 1965, Sara [141] investigated the Hf-C phase diagram by metallography and X-ray diffraction. The most refractory composition was established at $\text{HfC}_{0.90}$, with a melting temperature of 3830 °C. In 1967 Rudy and Progulski [143] determined the melting temperature to be 3928 ± 40 °C at $\text{HfC}_{0.942}$. In the same year, Deardorff et al. [144] found that hafnium carbide with stoichiometry from $\text{HfC}_{0.96}$ to HfC melts at ~ 3840 °C corroborating Sara's results [141], and Storms [21] reported HfC melting temperature at 3950 °C which is within the range of Rudy's measurements [143].

In 2016, new measurements of the melting temperature of hafnium carbide were performed, for the first time in the last fifty years. From laser melting experiments, Cedillos-Barraza et al. [145] reported the value 4232 ± 84 K (3959 °C) for $\text{HfC}_{0.98}$ composition. The latest experimental measurement was performed by Sheindlin et al. (2018) [62] (also by laser melting) and yielded similar value (3982 ± 30 °C) for close to stoichiometric HfC. These latest determinations overlap within reported uncertainties with 1967 measurements by Rudy and Progulski (3928 ± 40 °C) performed by Joule heating with Pirani furnace [143].

A computational study of high temperature thermodynamics of Hf-C, Hf-C-N, and Hf-Ta-C systems was reported by Hong and van de Walle in 2015 [1] using density functional theory (DFT) [146]. While the computational methods used are found to reliably predict trends in melting points as a function of composition, obtaining absolute melting points is more challenging. To assess the sensitivity of the results to the choice of exchange-correlation functional, they considered both the standard Perdew-Burke-Ernzerhof (PBE) functional [147] and the more accurate (but more computationally expensive) hybrid Heyd-Scuseria-Ernzerhof (HSE) functional [148], the latter being implemented perturbatively, for computational efficiency purposes. The highest melting point located at the $\text{HfC}_{0.81}$ composition was found to be of 3962 K (3689 °C) using PBE and 4422 K (4149 °C) using HSE. The true melting point should be closer to the HSE value but the difference in the two values is an indication of the order of magnitude of accuracy. Previous experimental values are indeed found to lie within the range spanned by the PBE and the HSE values.

In the Hf-Ta-C system, PBE values for melting temperature of Ta_4HfC_5 and HfC were found to be within computational uncertainties; however, in the Hf-C-N system, the pronounced maximum in melting temperature was discovered [1]. The highest melting point was predicted to be 4126 K (3853 °C) at the composition $\text{Hf}_{0.53}\text{C}_{0.27}\text{N}_{0.20}$, based on the PBE functional [1]. Compared to the PBE melting point of 3962 K in the Hf-C system, the Hf-C-N system further increases the melting point by 160 K (Figure 5). As predicted composition trends are more reliable than absolute numbers, these results suggest that the true melting point of $\text{Hf}_{0.53}\text{C}_{0.27}\text{N}_{0.20}$ is best estimated by adding 160 K to known experimental result for the Hf-C system. Taking experimental melting temperature for HfC as 3888–4012 °C (lower and upper limits from Rudy and Progulski [143] and Sheindlin et al. [62]), the melting temperature at $\text{Hf}_{0.53}\text{C}_{0.27}\text{N}_{0.20}$ is thus estimated at 4048–4172 °C which makes it a material with highest known melting point.

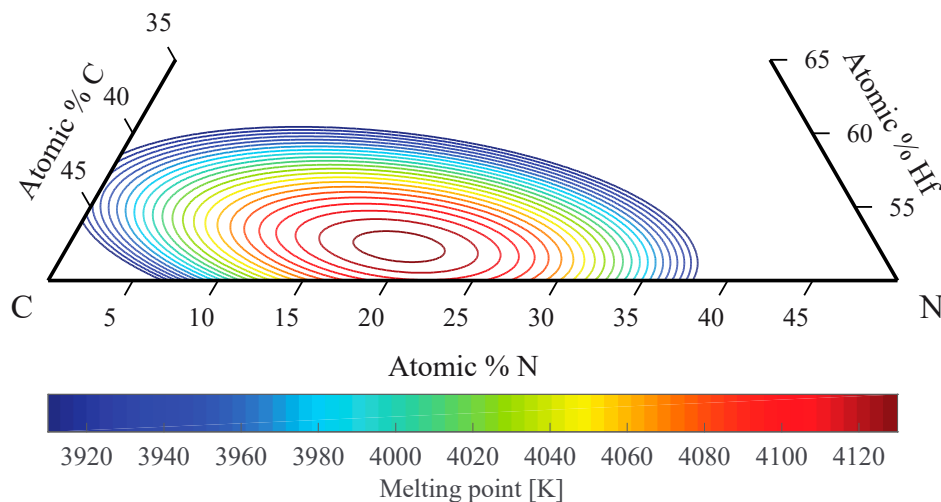


Figure 5. Melting temperatures of Hf-C-N alloys, based on density functional theory (DFT) calculations. Melting temperature maximum is located at $\text{Hf}_{0.53}\text{C}_{0.27}\text{N}_{0.20}$. Modified after Hong and van de Walle [1].

4.4. Thermochemistry

Standard enthalpies of formation, entropies and heat capacities for rocksalt carbides and nitrides of Zr and Hf are listed in Table 1. The values for Ti compounds are also shown for comparison.

4.4.1. Enthalpies of Formation

Enthalpies of formation of Zr and Hf carbides and Zr nitride were determined by several groups using combustion calorimetry in oxygen bomb. Due to differences in reported values for Zr carbides, Kornilov et al. in 1975 [136] performed a new experimental study on seven samples of $\text{ZrC}_{0.72}$ to $\text{ZrC}_{0.99}$ (Figure 6) and found close agreement with the 1969 work by Baker, Storms and Holley [149]. The same group reported new measurements on the formation enthalpy of hafnium carbide in 1977 [125].

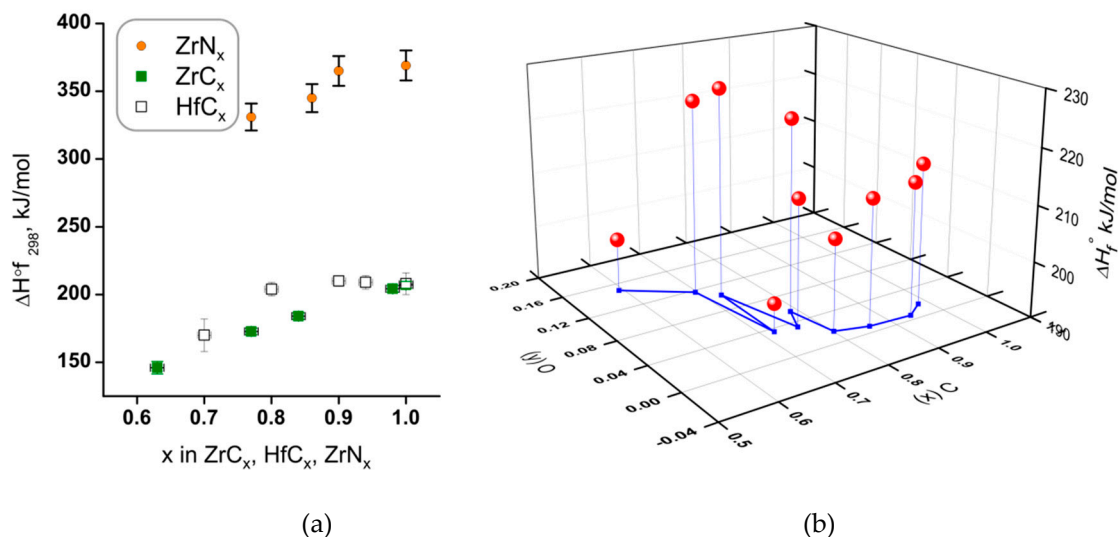


Figure 6. (a) Standard enthalpies of formation of Zr and Hf carbides and Zr nitrides as a function of carbon content. (b) Standard enthalpies of formation of 10 hafnium oxycarbides HfC_xO_y plotted measured by Kornilov et al. [125], from which the values for HfC_x were derived. Note that the oxygen content reaches $y = 0.15$ for most carbon deficient composition. See Tables S3 and S4 for reported uncertainties.

Table 2. Selected thermodynamic properties for rocksalt carbides and nitrides of Ti, Zr, and Hf: lattice parameters, enthalpies of formation, bond dissociation energies, standard entropies, heat capacities, melting temperatures, and thermal expansion coefficients.

	Lattice parameter a, Å [35]	ΔH_f^{298} kJ/mol [150]	D_0 kJ/mol [150]	S_{298} J/mol/K [150]	C_{p298} J/mol/K [150]	C_{p2000} J/mol/K [30]	T _m , °C	α 10 ^{−6} /K [23]
TiC	4.33	−209 ± 21 §	1388 ± 20	24.7 ± 0.2	34.3 ± 0.3	60.5	3067 ± 25 [143]	7.4
TiN	4.24	−338 ± 4	1261	30.3 ± 0.2	37.1 ± 0.1	61.2	2945 ± 30 [151]	9.3
ZrC	4.70	−207 ± 3	1508 ± 7	33.3 ± 0.1	37.9 ± 0.8	55.4	3572 ± 30 [62]	6.7
ZrN	4.57	−372 ± 2 †	1438 ± 6	38.9 ± 0.2	40.4 ± 0.1	57.3	2955 ± 30 [151]	7.2
HfC	4.64	−208 ± 8	1537 ± 9	40.1 ± 0.2	38.1 ± 0.2	50.2§	3982 ± 30 [62]	6.6
HfN	4.52	−374 ± 2 ‡	1461 ± 5	45 ± 1	41 ± 2	55.8 *	3330 ± 50 [151] §	6.9

|| cf. C_{p2000} 56.3 J/mol/K for $ZrC_{0.96}$ from Storms [21,22] and 57.4 J/mol/K for ZrC from NIST-JANAF [152]; § cf. ΔH_{f298} (TiC) −186 ± 18 from Meschel and Kleppa (2001) [153]; † cf. ΔH_{f298} (ZrN) −350 kJ/mol from Calphad optimization [91]; ‡ cf. ΔH_{f298} (HfN) 369.2 ± 1.4 kJ/mol from original work [93]; § refers to $HfC_{0.93}O_{0.07}$, cf. C_{p2000} ($HfC_{0.98}$) 57.1 J/mol/K from Storms [21,22]; * The value refers to $HfN_{0.93}O_{0.07}$ [30]; § T_m (HfN) was reported to increase with N pressure from 2920 °C at 0.01 atm to 3810 °C at 80 atm [59].

The value of the formation enthalpy of ZrN included in a Glushko's reference book (371.5 ± 1.2 kJ/mol) is consistent with the latest measurements performed by Galbraikh et al. [92] for stoichiometry ranging from $ZrN_{0.77}$ to ZrN. They have also measured the formation enthalpy for one oxynitride (see Tables S2 and S3 in supporting information for all compositions). In the latest optimization for Zr-N system, Sridar et al. [91] tabulate all the experimental values, varying from −336 to −365 kJ/mol. They also obtained the new value −341 kJ/mol by ab initio methods and arrived at a value of −350 kJ/mol based on a Calphad optimization.

There is a single measurement of formation enthalpy of HfN reported by Humphrey in 1953 [93]. He reports ΔH_{f298} as 369.2 ± 1.4 kJ/mol from eight measurements of heats of combustion, using ~5 g of HfN in each experiment. Samples were prepared by nitridation of metallic Hf at 1400–1500 °C; the lattice parameter was not measured, and a HfN stoichiometry was confirmed from weight gains on nitridation and combustion. In the same work, Humphrey also reported measurements of the formation enthalpy of HfO_2 , which is within 5 kJ/mol from currently accepted value [154]. Thus, we conclude that despite the fact that no new measurements on HfN were made for 60 years; there is no reason to suspect gross errors in HfN formation enthalpy reported by Humphrey [93]. No value for HfN formation enthalpy is included in the NIST-JANAF Thermochemical Tables [152]. The value for HfN given in Glushko's Thermal Constants of Substances [150] is −373.6 kJ/mol, and apparently includes minor adjustment in treatment of original data by Humphrey [93], which is the only source cited.

A systematic error is likely affecting data on formation enthalpies from combustion calorimetry on Hf and Zr metals, carbides, and nitrides. This should be kept in mind when comparing experimental data with ab initio calculations [155]. It comes from neglecting the contribution of surface energy of fine grained (nanophase) monoclinic HfO_2 and ZrO_2 formed as combustion products. The value for surface energy of monoclinic HfO_2 was unknown at the time of combustion calorimetry experiments. However, recent experimental results found the value 3.7 J/m² and accounting for it can change formation enthalpy measured by combustion experiments by as much as −20 kJ/mol [156].

4.4.2. High Temperature Heat Capacities from Calorimetry

Ti, Zr, and Hf nitrides have slightly higher heat capacities than carbides (Table 2). The evaluations for ZrC and ZrN in NIST-JANAF Thermochemical tables [152] are of 1964 vintage with no data for Hf analogs. The later evaluation by Storms [21] for $ZrC_{0.96}$ and $HfC_{0.98}$ are well known [22,81]. Turchanin et al. [30–32] measured high temperature enthalpies for Zr, and Hf carbonitrides by drop calorimetry and derived heat capacities with an estimated uncertainty of 1.5 %. His results are shown in Figure 7 and summarized below.

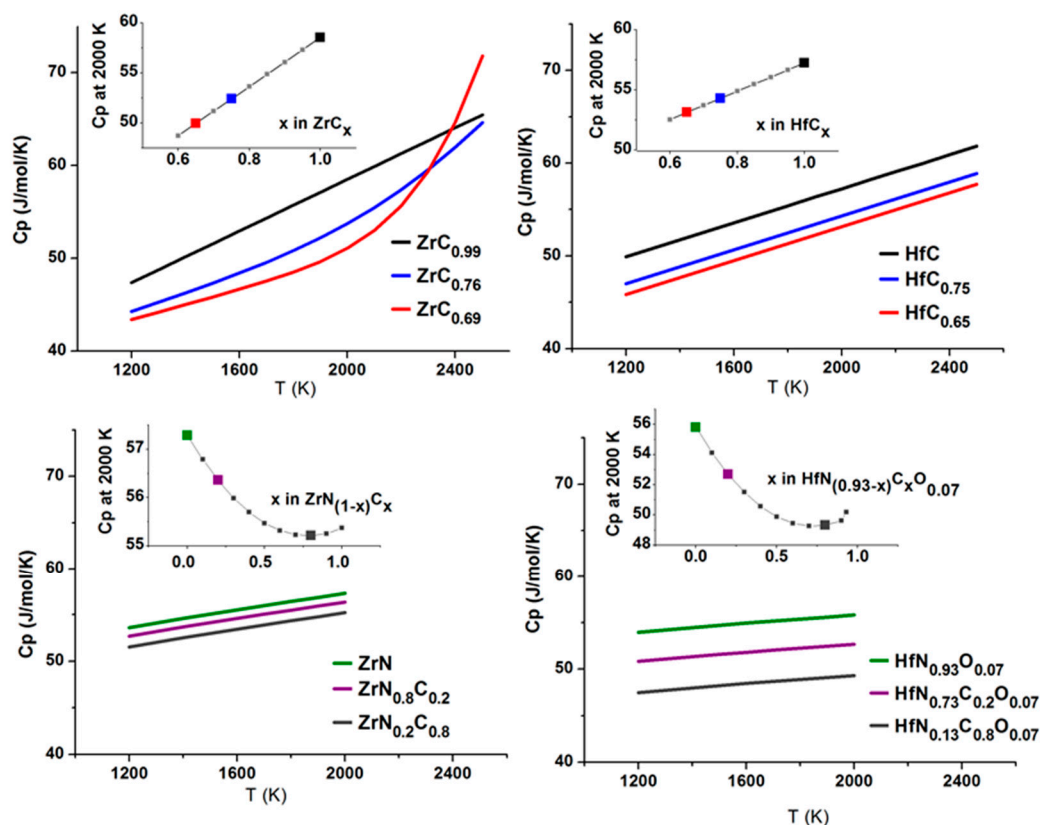


Figure 7. High temperature heat capacity (C_p) of zirconium and hafnium carbides and carbonitrides after Turchanin (1991) [30]. The insets show isotherms of heat capacity at 2000 K versus composition. Temperature dependence for selected compositions is shown on the main graphs. The data are tabulated in supporting information (Tables S6 and S7).

Turchanin's measurements were performed on samples 3–7 g in weight under high vacuum ($\sim 6 \cdot 10^{-6}$ Torr). The enthalpy increments were measured to 2227 °C (2500 K) for ZrC_x and HfC_x and to 1727 °C (2000 K) for $ZrN_{1-x}C_x$ and $HfN_{1-x}C_x$. All hafnium carbonitride samples studied by Turchanin were prepared from a mixture of carbides and nitrides at 2200–2800 °C and contained some oxygen and tabulated data are related to oxycarbonitrides with composition $HfN_{(0.93-x)}C_xO_{0.07}$. Heat capacity per mole of ZrC_x and HfC_x increases linearly with x , as expected due to the increasing total number of atoms per mole of compound. For carbon deficient zirconium carbides, Turchanin found that the C_p increase with temperature deviates from a linear behavior above ~ 1800 °C. This effect is likely related to the thermally activated motion of carbon atoms, so-called “sublattice melting” [157,158]. Turchanin did not observe this change in the rate of heat capacity increase for defective hafnium carbide. However, that does not indicate that this effect is absent in HfC_{1-x} ; its melting temperature is ~ 400 °C higher than for zirconium carbide and the effect may not appear in the lower temperature range of the measurements (below 2227 °C).

For the carbonitrides, $ZrN_{1-x}C_x$ and $HfN_{1-x}C_x$, the heat capacity decreases with carbon content, but not linearly, with a minimum in C_p for a composition of $x = 0.8$. Turchanin notes that this minimum corresponds to the composition with the strongest bonding since, in carbonitrides, the electronic contribution to heat capacity does not change substantially.

Lengauer et al. [40] studied the heat capacities of several Hf and Zr carbonitride compositions by differential scanning calorimetry (DSC) below 1000 °C and reported good agreement with the corresponding Turchanin values for Zr carbonitrides, although the limited number of compositions in Lengauer's study did not allow him to confirm the minimum in C_p reported by Turchanin. Recently, Ciriello et al. [6] performed measurements of the heat capacity of pure ZrN from 1.8 K, as part of

a study of the thermal conductivity of (ZrPu)N solid solutions. Their C_p value for ZrN at 1200 °C (52 J/mol/K) is in good agreement with Turchanin's evaluation (Table 2).

4.4.3. Fusion Enthalpies of ZrC and ZrN from Pulsed Heating

The method of pulsed heating [74,159,160] originated from the “exploding wire” technique [160] and was extremely useful for the determination of high temperature resistivities, heat capacities, and fusion enthalpies of metals. It relies on the pyrometric measurement of sample temperature increase on capacitors discharges through the metal wire. Due to the microseconds timeframe of discharge, the heat losses can be neglected, and the total energy is known from the capacitor calibration. Recently, this approach was successfully applied for carbides and nitrides films 100 μm or thinner [61,63–66,161,162] and the first experimental data on fusion enthalpies and high temperature heat capacities of ZrC and ZrN were reported. The fusion enthalpy of ZrN was measured as 104 kJ/mol [65], and the fusion enthalpy of ZrC_x was found to increase from 92 kJ/mol for ZrC to 111 kJ/mol for $\text{ZrC}_{0.95}$. The experimental setup described by Savvatimskiy et al. [63] provides black body-like geometry for measurements by a sighting pyrometer inside the wedge formed by glass plates coated with the sample. We expect that future applications of the “exploding wire” technique to metallic nitrides and carbides will result in an explosion in much needed thermodynamic data for Calphad modeling of carbonitride systems and for testing the predictions of ab initio computations.

4.4.4. Fusion Enthalpies of HfC–HfN from ab Initio Computations

Based on DFT calculations by Hong and van de Walle (2015) [1], HfC_x has an exceptionally large fusion enthalpy, as high as 0.81 eV/atom. This is a value unparalleled among refractories. (For reference, Al_2O_3 (m.p. 2345 K): 0.22; W (m.p. 3695 K): 0.37; Hf (m.p. 2506 K): 0.26 eV/atom). Estimated fusion enthalpies of HfC_x and HfC_xN_y are summarized in Table 3. Note that these fusion enthalpies were obtained as a byproduct in the process of melting temperature calculation [1], using the small-size coexistence method [163]. As a result, they were slightly underestimated, due to high defect concentration in the freshly formed solid phase. A more accurate method, which models the solid and liquid phases in separate simulations, typically increases the fusion enthalpy by 0.05–0.10 eV/atom in these systems.

Table 3. Fusion enthalpies of HfC_x and HfC_xN_y from DFT calculations [1].

HfC_x	Fusion Enthalpy		HfC_xN_y	Fusion enthalpy	
	(eV/atom)	(kJ/mol)		(eV/atom)	(kJ/mol)
HfC	0.67	130	$\text{HfC}_{0.75}\text{N}_{0.22}$	0.79	150
$\text{HfC}_{0.97}$	0.68	130	$\text{HfC}_{0.62}\text{N}_{0.19}$	0.71	124
$\text{HfC}_{0.94}$	0.76	141	$\text{HfC}_{0.56}\text{N}_{0.25}$	0.73	127
$\text{HfC}_{0.91}$	0.72	133	$\text{HfC}_{0.56}\text{N}_{0.38}$	0.75	141
$\text{HfC}_{0.88}$	0.73	131	$\text{HfC}_{0.44}\text{N}_{0.5}$	0.74	139
$\text{HfC}_{0.84}$	0.73	130	$\text{HfC}_{0.31}\text{N}_{0.62}$	0.69	130
$\text{HfC}_{0.81}$	0.72	126			
$\text{HfC}_{0.78}$	0.69	118			
$\text{HfC}_{0.75}$	0.69	117			

While there is no experimental fusion enthalpy of HfC_x for comparison, the computational value, 0.81 eV/atom or 147 kJ/mol, is consistent with the experimental values of the fusion enthalpy of ZrC_x from pulse heating experiments reviewed above, given that the melting temperature of ZrC_x (3572 °C) is lower than that of HfC_x (3982 °C) by 10%.

5. Summary and Future Directions

Despite the sharp increase in the number of publications on carbides, the literature's focus has been on either widely used Ti carbonitrides, or on multicomponent (so-called high entropy) compositions, and large areas remain to be mapped computationally and experimentally. For instance, no thermodynamic optimization for the Hf-N system has been performed. Only isothermal crosssections were assessed for the Hf-C-O and Zr-C-O and Hf-C-N and Zr-C-N systems, and there are conflicting experimental results on oxygen solubility in HfC and ZrC. This points to a critical need for fundamental data to be further integrated into suitable thermodynamic models. Oxidation behavior and interaction with water vapor is of paramount importance for the use of carbides in high temperature flight and fission reactors related applications, yet limits of oxygen and hydrogen solubility in Zr and Hf carbides and nitrides are not reliably established as a function of temperature.

Prompted by the recent prediction of highest melting temperature in Hf-C-N system [1] we screened the literature for possible experimental evidence and found two reports indicating that some compositions of Hf(C,N) solid solution might indeed have higher bonding strength than end members: (i) Brundiers in 1975 [126] reported that the $\text{HfC}_{0.58}\text{N}_{0.42}$ composition had the highest hardness and smallest thermal expansion in the Hf-C-N system; (ii) Turchanin in 1991 [30] reported minima in heat capacities isotherms for Hf(C,N) and Zr(C,N) compositions. Since the electronic contribution to the heat capacity should not vary much from carbides to nitrides, the difference is likely coming primarily from lattice vibrations and compositions with the heat capacity minima are associated with higher-frequency phonon spectra and thus the strongest bonds [164].

Brunder's [126] work is a PhD thesis published in German, and Turchanin's predictions [30] were published in a monograph in Russian. It is thus no surprise that they mostly escaped attention until now. Still, a direct experimental confirmation of the high melting points predicted in the Hf-C-N system [1] would be welcome. In addition, as high melting temperature correlates with high hardness, a study of Zr and Hf carbonitrides may provide coatings superior to Ti carbonitrides currently used.

Supplementary Materials: The following are available online at <http://www.mdpi.com/1996-1944/12/17/2728/s1>, Table S1: The selected reactions for preparation of carbides and nitrides of Zr and Hf; Table S2: Unit cell parameters for NaCl-type compounds reported in Hf-Zr-C-O-N system; Figure S1: Dependence of unit cell parameters of substoichiometric Zr and Hf carbides from carbon content; Table S3: Standard enthalpies of formation of HfC_xO_y compounds; Table S4: Standard enthalpies of formation of ZrN_xO_y compounds; Table S5: Heat capacities of Zr and Hf carbides; Table S6: Heat capacities of Zr carbonitrides; Table S7: Heat capacities of Hf carbonitrides; Figure S2: Compositions of NaCl-type hafnium carbonitrides in Hf-C-N system at 1500 °C and 1 atm N_2 .

Author Contributions: Writing-Original Draft Preparation, S.V.U and Q.-J.H.; Writing-Review & Editing, A.N. and A.v.d.W.; Visualization, S.V.U and Q.-J.H.

Funding: The work was supported by the National Science Foundation under Collaborative Research Awards DMR-1835848 (UC Davis) and DMR-1835939 (Brown University).

Acknowledgments: The work was supported by the National Science Foundation under Collaborative Research Awards DMR-1835848 (UC Davis) and DMR-1835939 (Brown University). S.V.U. gratefully acknowledges consultation with G.S. Upadhyaya.

Conflicts of Interest: The authors declare no conflict of interest.

References

1. Hong, Q.-J.; van de Walle, A. Prediction of the material with highest known melting point from ab initio molecular dynamics calculations. *Phys. Rev. B* **2015**, *92*, 020104. [CrossRef]
2. Searcy, A.W.; Ragone, D.V.; Colombo, U.; Donegani, F. *Chemical and Mechanical Behavior of Inorganic Materials*; Wiley-Interscience: Hoboken, NJ, USA, 1970.
3. Ettmayer, P.; Lengauer, W. *Ullmann's Encyclopedia of Industrial Chemistry*; Wiley: Weinheim, Germany, 2012; Volume 24.
4. Watson, C.W. *Nuclear Rockets: High-Performance Propulsion for Mars*; LA-12784-MS; Los Alamos National Laboratory: Los Alamos, NM, USA, 1994; INIS Volume 25, Available online: [Inis.iaea.org/search/search.aspx?orig_q=RN:25070120](https://inis.iaea.org/search/search.aspx?orig_q=RN:25070120) (accessed on 23 August 2019).

5. Katoh, Y.; Vasudevamurthy, G.; Nozawa, T.; Snead, L.L. Properties of zirconium carbide for nuclear fuel applications. *J. Nucl. Mater.* **2013**, *441*, 718–742. [[CrossRef](#)]
6. Ciriello, A.; Rondinella, V.V.; Staicu, D.; Somers, J.; Benes, O.; Jardin, R.; Bouexiere, D.; Wastin, F.; Colineau, E. Thermophysical characterization of ZrN and (Zr, Pu)N. *J. Alloys Compd.* **2009**, *473*, 265–271. [[CrossRef](#)]
7. Berg, G.; Friedrich, C.; Broszeit, E.; Berger, C. Data Collection of Properties of Hard Material. In *Handbook of Ceramic Hard Materials*; Riedel, R., Ed.; Wiley: Darmstadt, Germany, 2000. [[CrossRef](#)]
8. Hans, K.; Latha, S.; Bera, P.; Barshilia, H.C. Hafnium carbide based solar absorber coatings with high spectral selectivity. *Sol. Energy Mater. Sol. Cells* **2018**, *185*, 1–7. [[CrossRef](#)]
9. Chung, S.; Shrestha, S.; Wen, X.; Feng, Y.; Gupta, N.; Xia, H.; Yu, P.; Tang, J.; Conibeer, G. Hafnium nitride for hot carrier solar cells. *Sol. Energy Mater. Sol. Cells* **2016**, *144*, 781–786. [[CrossRef](#)]
10. Xu, J.; Xu, S.; Munroe, P.; Xie, Z.-H. A ZrN nanocrystalline coating for polymer electrolyte membrane fuel cell metallic bipolar plates prepared by reactive sputter deposition. *RSC Adv.* **2015**, *5*, 67348–67356. [[CrossRef](#)]
11. Randhawa, H. Hard coatings for decorative applications. *Surf. Coat. Technol.* **1988**, *36*, 829–836. [[CrossRef](#)]
12. Klumdoung, P.; Buranawong, A.; Chaiyakun, S.; Limsuwan, P. Variation of color in zirconium nitride thin films prepared at high Ar flow rates with reactive dc magnetron sputtering. *Procedia Eng.* **2012**, *32*, 916–921. [[CrossRef](#)]
13. Zheng, C.Y.; He, G.; Chen, X.F.; Liu, M.; Lv, J.G.; Gao, J.; Zhang, J.W.; Xiao, D.Q.; Jin, P.; Jiang, S.S.; et al. Modification of band alignments and optimization of electrical properties of in GaZnO MOS capacitors with high-k HfOxNy gate dielectrics. *J. Alloys Compd.* **2016**, *679*, 115–121. [[CrossRef](#)]
14. Wallace, R.M.; Stoltz, R.A.; Wilk, G.D. Fabricating a Field-Effect Device Having a Zirconium and/or Hafnium Oxynitride Gate Dielectric and Integrated Circuit Using the Device. US Patent US6013553A, 11 January 2000.
15. Tsai, L.-S.; Wang, C.-H.; Chen, W.-Y.; Wang, W.-C.; Hwang, J.-C. Low-voltage organic thin-film transistors with hydrophobic hafnium oxynitride film as gate insulator. *Org. Electron.* **2010**, *11*, 123–126. [[CrossRef](#)]
16. Thangadurai, P.; Mikhelashvili, V.; Eisenstein, G.; Kaplan, W.D. Microstructure and chemical analysis of Hf-based high-k dielectric layers in metal-insulator-metal capacitors. *Thin Solid Film.* **2010**, *518*, 4467–4472. [[CrossRef](#)]
17. Skaja, K.; Schönbohm, F.; Weier, D.; Lühr, T.; Keutner, C.; Berges, U.; Westphal, C. Thermal stability of an ultrathin hafnium oxide film on plasma nitrided Si(100). *Surf. Sci.* **2013**, *616*, 104–109. [[CrossRef](#)]
18. Fahrenholtz, W.G.; Hilmas, G.E. Ultra-high temperature ceramics: Materials for extreme environments. *Scr. Mater.* **2017**, *129*, 94–99. [[CrossRef](#)]
19. Fahrenholtz, W.G.; Wuchina, E.J.; Lee, W.E.; Zhou, Y. *Ultra-High Temperature Ceramics: Materials for Extreme Environment Applications*; Wiley: Hoboken, NJ, USA, 2014.
20. Goldschmidt, H.J. *Interstitial Alloys*; Butterworth Co.: London, UK, 1967.
21. Storms, E. *The Refractory Carbides*; Academic Press: New York, NY, USA, 1967; p. 144.
22. Toth, L. *Transition Metal Carbides and Nitrides*; Academic Press: New York, NY, USA; London, UK, 1971.
23. Pierson, H.O. *Handbook of Refractory Carbides and Nitrides: Properties, Characteristics, Processing, and Applications*; William Andrew: Norwich, NY, USA, 1996.
24. Freer, R. *The Physics and Chemistry of Carbides, Nitrides and Borides*; Springer: Dordrecht, The Netherlands, 1990; Volume 185.
25. Samsonov, G.V. *Refractory Carbides*; Springer: Boston, MA, USA, 1995.
26. Oyama, S.T. *The Chemistry of Transition Metal Carbides and Nitrides*; Springer: Dordrecht, The Netherlands, 1996.
27. Gogotsi, Y.G.; Andrievski, R.A. *Materials Science of Carbides, Nitrides and Borides*; Springer: Dordrecht, The Netherlands, 1999; Volume 68.
28. Levy, R.B. Properties of Carbides, Nitrides and Borides: Implications for Catalysis. In *Advanced Materials in Catalysis*; Burton, J.J., Garten, R.L., Eds.; Academic Press: New York, NY, USA, 1977; pp. 101–127.
29. Ham, D.; Lee, J. Transition Metal Carbides and Nitrides as Electrode Materials for Low Temperature Fuel Cells. *Energies* **2009**, *2*, 873. [[CrossRef](#)]
30. Turchanin, A.G.; Turchanin, M.A. *Thermodynamics of Refractory Carbides and Carbonitrides*; Metallurgiya: Moscow, Russia, 1991; p. 352. (In Russian)
31. Turchanin, A.G.; Babenko, S.A. Thermodynamic properties of zirconium carbonitride (ZrC_xN_{1-x}) at 298–1500 K. *Izv. Akad. Nauk SSSR Neorg. Mater.* **1985**, *21*, 1325–1328.
32. Turchanin, A.G.; Babenko, S.A.; Mitrofanov, B.V.; Ivenko, N.V. Thermodynamic properties of hafnium oxycarbonitride at 298–1500 K. *Zh. Fiz. Khim.* **1985**, *59*, 1847–1849.

33. Turchanin, A.G.; Fesenko, V.V. Enthalpy and heat capacity of zirconium carbide in the homogeneity region over the temperature range 1300–2500 K. *Poroshk. Metall.* **1968**, *8*, 88–90.
34. Turchanin, A.G.; Polyakov, A.E. Thermodynamic properties of hafnium carbide in the 0–3000 K range. *Izv. Akad. Nauk SSSR Neorg. Mater.* **1982**, *18*, 404–406.
35. Samsonov, G.V.; Upadhyaya, G.S.; Neshpor, V.S. *Physical Materials Science of Carbides*; Naukova Dumka: Kiev, Ukraine, 1974. (In Russian)
36. Upadhyaya, G.S. *Nature and Properties of Refractory Carbides*; Nova Science Publishers: Commack, NY, USA, 1996; p. 545.
37. Lengauer, W. Multiphase reaction diffusion in transition metal-carbon and transition metal-nitrogen systems. *J. Alloys Compd.* **1995**, *229*, 80–92. [[CrossRef](#)]
38. Lengauer, W. Transition Metal Carbides, Nitrides, and Carbonitrides. In *Handbook of Ceramic Hard Materials*; Riedel, R., Ed.; Wiley-VCH: Weinheim, Germany, 2000; pp. 202–252.
39. Lengauer, W. Carbides: Transition Metal Solid-State Chemistry. In *Encyclopedia of Inorganic and Bioinorganic Chemistry*; John Wiley Sons Ltd.: Hoboken, NJ, USA, 2012. [[CrossRef](#)]
40. Lengauer, W.; Binder, S.; Aigner, K.; Ettmayer, P.; Guillou, A.; Debuigne, J.; Groboth, G. Solid state properties of group IVb carbonitrides. *J. Alloys Compd.* **1995**, *217*, 137–147. [[CrossRef](#)]
41. Lengauer, W.; Bohn, M. Thermochemical Basis of the Preparation of Well-Defined Transition Metal Carbide, Nitride and Carbonitride Reference Materials for Electron-Probe Microanalysis (EPMA). *Solid State Prop. Nitrides Carbonitrides Carbonitride-Based Cermets* **2018**, *274*, 20. [[CrossRef](#)]
42. Shabalin, I.L. *Ultra-High Temperature Materials II: Refractory Carbides I (Ta, Hf, Nb and Zr Carbides)*; Springer: Dordrecht, The Netherlands, 2019. [[CrossRef](#)]
43. Juza, R.; Rabenau, A.; Nitschke, I. Über ein braunes Zirkonnitrid Zr_3N_4 . *Z. Anorg. Allg. Chem.* **1964**, *332*, 1–4. [[CrossRef](#)]
44. Lerch, M.; Füglein, E.; Wrba, J. Synthesis, Crystal Structure, and High Temperature Behavior of Zr_3N_4 . *Z. Anorg. Allg. Chem.* **1996**, *622*, 367–372. [[CrossRef](#)]
45. Zerr, A.; Miehe, G.; Riedel, R. Synthesis of cubic zirconium and hafnium nitride having Th_3P_4 structure. *Nat. Mater.* **2003**, *2*, 185–189. [[CrossRef](#)]
46. Schwarz, K.; Williams, A.R.; Cuomo, J.J.; Harper, J.H.E.; Hentzell, H.T.G. Zirconium nitride—A new material for Josephson junctions. *Phys. Rev. B Condens. Matter* **1985**, *32*, 8312–8316. [[CrossRef](#)]
47. Johansson, B.O.; Hentzell, H.T.G.; Harper, J.M.E.; Cuomo, J.J. Higher nitrides of hafnium, zirconium, and titanium synthesized by dual ion beam deposition. *J. Mater. Res.* **1986**, *1*, 442–451. [[CrossRef](#)]
48. Tsuchida, T.; Kawaguchi, M.; Kodaira, K. Synthesis of ZrC and ZrN in air from mechanically activated Zr-C powder mixtures. *Solid State Ion.* **1997**, *101–103*, 149–154. [[CrossRef](#)]
49. Lerch, M. Nitridation of zirconia. *J. Am. Ceram. Soc.* **1996**, *79*, 2641–2644. [[CrossRef](#)]
50. Yamamura, H.; Emoto, S.; Mori, T. Factors affecting the formation rate of ZrN by the carbothermal nitridation method. *J. Ceram. Soc. Jpn.* **1998**, *106*, 650–653. [[CrossRef](#)]
51. David, J.; Trolliard, G.; Volkringer, C.; Loiseau, T.; Masson, O.; Maitre, A. Study of the reaction mechanisms involved in the formation of zirconium oxycarbide from Metal-Organic Frameworks (MOFs) precursors. *J. Alloys Compd.* **2016**, *680*, 571–585. [[CrossRef](#)]
52. Yin, L.; Jones, M.I. Synthesis of ZrN powders by aluminum-reduction nitridation of ZrO_2 powders with $CaCO_3$ additive. *Ceram. Int.* **2017**, *43*, 3183–3189. [[CrossRef](#)]
53. Li, Y.; Li, N.; Ruan, G.; Li, J.; Li, X. Effects of technical factors on $MgAl_2O_4$ -TiN composites produced by aluminothermic reduction and nitridation. *Mater. Des.* **2006**, *28*, 969–972. [[CrossRef](#)]
54. Perry, A.J.; Schlapbach, L.; Sproul, W.D. Non-stoichiometry effects in the XPS spectra of HfN films. *Solid State Commun.* **1987**, *62*, 23–26. [[CrossRef](#)]
55. Réjasse, F.; Rapaud, O.; Trolliard, G.; Masson, O.; Maitre, A. Experimental investigation and thermodynamic evaluation of the C-O-Zr ternary system. *RSC Adv.* **2016**, *6*, 100122–100135. [[CrossRef](#)]
56. Samsonow, G.W.; Morosow, W.W. Carbohydride der Übergangsmetalle (ICSD 77008). *Mon. Chem./Chem. Mon.* **1971**, *102*, 1667–1678. [[CrossRef](#)]
57. Ma, X.; Li, C.; Bai, K.; Wu, P.; Zhang, W. Thermodynamic assessment of the Zr–N system. *J. Alloys Compd.* **2004**, *373*, 194–201. [[CrossRef](#)]
58. Fernández Guillermet, A. Analysis of thermochemical properties and phase stability in the zirconium-carbon system. *J. Alloys Compd.* **1995**, *217*, 69–89. [[CrossRef](#)]

59. Okamoto, H. The Hf-N (Hafnium-Nitrogen) system. *Bull. Alloy Phase Diagr.* **1990**, *11*, 146–149. [[CrossRef](#)]
60. Bittermann, H.; Rogl, P. Critical assessment and thermodynamic calculation of the binary system hafnium-carbon (Hf-C). *J. Phase Equilibria* **1997**, *18*, 344–356. [[CrossRef](#)]
61. Savvatimskiy, A.I.; Onufriev, S.V.; Muboyadzhy, S.A. Thermophysical properties of the most refractory carbide Ta_{0.8}Hf_{0.2}C under high temperatures (2000–5000 K). *J. Eur. Ceram. Soc.* **2019**, *39*, 907–914. [[CrossRef](#)]
62. Sheindlin, M.; Falyakhov, T.; Petukhov, S.; Valyano, G.; Vasin, A. Recent advances in the study of high-temperature behaviour of non-stoichiometric TaC_x, HfC_x and ZrC_x carbides in the domain of their congruent melting point. *Adv. Appl. Ceram.* **2018**, *117* (Suppl. 1), s48–s55. [[CrossRef](#)]
63. Savvatimskiy, A.I.; Onufriev, S.V.; Muboyajan, S.A.; Tsygankov, P.A. Pulsed Heating of Carbides. *Bull. Russ. Acad. Sci. Phys.* **2018**, *82*, 363–368. [[CrossRef](#)]
64. Savvatimskiy, A.I.; Onufriev, S.V.; Muboyadzhy, S.A. Measurement of ZrC properties up to 5000 K by fast electrical pulse heating method. *J. Mater. Res.* **2017**, *32*, 1287–1294. [[CrossRef](#)]
65. Onufriev, S.V.; Kondratiev, A.M.; Savvatimskiy, A.I.; Val'vano, G.E.; Muboyajan, S.A. Investigation of the high-temperature properties of zirconium nitride by impulse current heating method. *High Temp.* **2015**, *53*, 455–457. [[CrossRef](#)]
66. Kondratyev, A.; Muboyajan, S.; Onufriev, S.; Savvatimskiy, A. The application of the fast pulse heating method for investigation of carbon-rich side of Zr–C phase diagram under high temperatures. *J. Alloys Compd.* **2015**, *631*, 52–59. [[CrossRef](#)]
67. Lv, Z.; Hu, H.; Wu, C.; Cui, S.; Zhang, G.; Feng, W. First-principles study of structural stability, electronic and elastic properties of ZrC compounds. *Phys. B Condens. Matter* **2011**, *406*, 2750–2754. [[CrossRef](#)]
68. Weinberger, C.R.; Thompson, G.B. Review of phase stability in the group IVB and VB transition-metal carbides. *J. Am. Ceram. Soc.* **2018**, *101*, 4401–4424. [[CrossRef](#)]
69. Weinberger, C.R.; Yu, H.; Wang, B.; Thompson, G.B. A computational investigation into the microstructures and stability of the zeta phase in transition metal carbides and nitrides. *Adv. Appl. Ceram.* **2018**, *117* (Suppl. 1), s26–s33. [[CrossRef](#)]
70. Van de Walle, A.; Sun, R.; Hong, Q.-J.; Kadkhodaei, S. Software tools for high-throughput CALPHAD from first-principles data. *Calphad* **2017**, *58*, 70–81. [[CrossRef](#)]
71. Sundman, B.; Kattner, U.R.; Palumbo, M.; Fries, S.G. OpenCalphad—A free thermodynamic software. *Integr. Mater. Manuf. Innov.* **2015**, *4*. [[CrossRef](#)]
72. Liu, Z.-K. First-Principles Calculations and CALPHAD Modeling of Thermodynamics. *J. Phase Equilibria Diffus.* **2009**, *30*, 517. [[CrossRef](#)]
73. Kaufman, L.; Ågren, J. CALPHAD, first and second generation—Birth of the materials genome. *Scr. Mater.* **2014**, *70*, 3–6. [[CrossRef](#)]
74. Gallob, R.; Jaeger, H.; Pottlacher, G. A submicrosecond pulse heating system for the investigation of thermophysical properties of metals at high temperatures. *Int. J. Thermophys.* **1986**, *7*, 139–147. [[CrossRef](#)]
75. Froberg, M.G. Thirty years of levitation melting calorimetry—A balance. *Thermochim. Acta* **1999**, *337*, 7–17. [[CrossRef](#)]
76. Dinsdale, A.T. SGTE data for pure elements. *Comput. Coupling Phase Diagr. Thermochem.* **1991**, *15*, 317–425. [[CrossRef](#)]
77. Luo, A.A. Material design and development: From classical thermodynamics to CALPHAD and ICME approaches. *Calphad* **2015**, *50*, 6–22. [[CrossRef](#)]
78. Olson, G.B.; Kuehmann, C.J. Materials genomics: From CALPHAD to flight. *Scr. Mater.* **2014**, *70*, 25–30. [[CrossRef](#)]
79. Sara, R.V. The system zirconium-carbon. *J. Am. Ceram. Soc.* **1965**, *48*, 243–247. [[CrossRef](#)]
80. Rudy, E. *Ternary Phase Equilibria in Transition Metal-Boron-Carbon-Silicon Systems. V. Compendium of Phase Diagram Data*; Aerojet-General Corp.: Sacramento, CA, USA, 1969; p. 731. Available online: www.osti.gov/biblio/4754828 (accessed on 23 August 2019).
81. Jackson, H.F.; Lee, W.E. Properties and characteristics of ZrC. In *Material Properties. Oxide Fuels for Light Water Reactors and Fast Neutron Reactors*; Konings, R.J.M., Ed.; Elsevier B.V.: Amsterdam, The Netherlands; Waltham, MA, USA, 2012; Volume 2, pp. 339–372. [[CrossRef](#)]
82. Zhou, P.; Peng, Y.; Du, Y.; Wang, S.; Wen, G. Thermodynamic modeling of the C-W-Zr system. *Int. J. Refract. Met. Hard Mater.* **2015**, *50*, 274–281. [[CrossRef](#)]

83. Pirani, M.; Alterthum, H. Method for the determination of the melting point of metals which fuse at high temperatures. *Z. Elektrochem. Angew. Phys. Chem.* **1923**, *29*, 5–8.
84. Okamoto, H. C-Hf (carbon-hafnium). *J. Phase Equilibria* **2001**, *22*, 510. [\[CrossRef\]](#)
85. Bittermann, H.; Rogl, P. Critical assessment and thermodynamic calculation of the ternary system C-Hf-Zr (carbon-zirconium-hafnium). *J. Phase Equilibria* **2002**, *23*, 218–235. [\[CrossRef\]](#)
86. Brukl, C.E.; Harmon, D.P. *Ternary Phase Equilibria in Transition Metal-Boron-Carbon-Silicon Systems. II. Ternary Systems. 4. Titanium-Zirconium-Carbon, Titanium-Hafnium-Carbon, and Zirconium-Hafnium-Carbon Systems*; CAN70:81391; Materials Research Laboratory, Aerojet-General Corp.: Sacramento, CA, USA, 1966; p. 92.
87. Adjaoud, O.; Steinle-Neumann, G.; Burton, B.P.; van de Walle, A. First-principles phase diagram calculations for the HfC-TiC, ZrC-TiC, and HfC-ZrC solid solutions. *Phys. Rev. B* **2009**, *80*, 134112. [\[CrossRef\]](#)
88. Obata, N.; Nakazawa, N. Superlattice formation in zirconium-carbon system. *J. Nucl. Mater.* **1976**, *60*, 39–42.
89. Hu, W.; Xiang, J.; Zhang, Y.; Liu, S.; Chen, C.; Wang, P.; Wang, H.; Wen, F.; Xu, B.; He, J.; et al. Superstructural nanodomains of ordered carbon vacancies in nonstoichiometric $\text{ZrC}_{0.61}$. *J. Mater. Res.* **2012**, *27*, 1230–1236. [\[CrossRef\]](#)
90. Domagala, R.F.; McPherson, D.J.; Hansen, M. System Zirconium-Nitrogen. *JOM* **1956**, *8*, 98–105. [\[CrossRef\]](#)
91. Sridar, S.; Kumar, R.; Hari Kumar, K.C. Thermodynamic modelling of Ti-Zr-N system. *Comput. Coupling Phase Diagr. Thermochem.* **2017**, *56*, 102–107. [\[CrossRef\]](#)
92. Gal'braikh, É.I.; Kulik, O.P.; Kuznetsov, A.A.; Lyutaya, M.D.; Morozova, M.P. Enthalpy of formation of the nitrogen solid solution in α -zirconium and of zirconium nitride in their homogeneity regions. *Sov. Powder Metall. Met. Ceram.* **1970**, *9*, 748–751. [\[CrossRef\]](#)
93. Humphrey, G.L. Heats of formation of hafnium oxide and hafnium nitride. *J. Am. Chem. Soc.* **1953**, *75*, 2806–2807. [\[CrossRef\]](#)
94. Rudy, E. Crystal structures of Hf_3N_2 and Hf_4N_3 . *Met. Trans.* **1970**, *1*, 1249–1252. [\[CrossRef\]](#)
95. Lengauer, W.; Rafaja, D.; Täubler, R.; Kral, C.; Ettmayer, P. Preparation of binary single-phase line compounds via diffusion couples: The subnitride phases $\eta\text{-Hf}_3\text{N}_{2-x}$ and $\zeta\text{-Hf}_4\text{N}_{3-x}$. *Acta Metall. Mater.* **1993**, *41*, 3505–3514. [\[CrossRef\]](#)
96. Xu, M.; Wang, S.; Yin, G.; Li, J.; Zheng, Y.; Chen, L.; Jia, Y. Optical properties of cubic Ti_3N_4 , Zr_3N_4 , and Hf_3N_4 . *Appl. Phys. Lett.* **2006**, *89*. [\[CrossRef\]](#)
97. Yablonskikh, M.; Dzivenko, D.; Bourguille, J.; Riedel, R.; Magnano, E.; Parmigiani, F.; Zerr, A. Electronic structure and band gap of oxygen bearing c- Zr_3N_4 and of c- Hf_3N_4 by soft X-ray spectroscopy. *Phys. Status Solidi A* **2014**, *211*, 835–842. [\[CrossRef\]](#)
98. Yu, S.; Zeng, Q.; Oganov, A.R.; Frapper, G.; Huang, B.; Niu, H.; Zhang, L. First-principles study of Zr-N crystalline phases: Phase stability, electronic and mechanical properties. *RSC Adv.* **2017**, *7*, 4697–4703. [\[CrossRef\]](#)
99. Zhang, J.-D.; Yang, K. Theoretical study of the thermodynamic properties of cubic Zr_3N_4 and Hf_3N_4 under high pressures. *J. Alloys Compd.* **2014**, *608*, 90–94. [\[CrossRef\]](#)
100. Zhang, J.-P.; Zhu, X.-L.; Zhang, Y.-Y.; Gao, J.-X. First principles study on structural and electronic properties and defect formation enthalpies of cubic Hf_3N_4 under high pressure. *Can. J. Phys.* **2014**, *92*, 1581–1586. [\[CrossRef\]](#)
101. Zheng, F.; Fang, Y.; Yu, S.; Wu, S.; Zhu, Z.-Z. Exploration of crystal structures and phase transitions in Hf_3N_4 . *CrystEngComm* **2017**, *19*, 2608–2613. [\[CrossRef\]](#)
102. Oganov, A.R.; Pickard, C.J.; Zhu, Q.; Needs, R.J. Structure prediction drives materials discovery. *Nat. Rev. Mater.* **2019**, *4*, 331–348. [\[CrossRef\]](#)
103. Zhang, J.; Oganov, A.R.; Li, X.; Niu, H. Pressure-stabilized hafnium nitrides and their properties. *Phys. Rev. B* **2017**, *95*, 020103. [\[CrossRef\]](#)
104. Gu, Z.; Hu, C.; Huang, H.; Zhang, S.; Fan, X.; Wang, X.; Zheng, W. Identification and thermodynamic mechanism of the phase transition in hafnium nitride films. *Acta Mater.* **2015**, *90*, 59–68. [\[CrossRef\]](#)
105. Sui, Y.R.; Xu, Y.; Yao, B.; Xiao, L.; Liu, B. Preparation, characterization and properties of N-rich Zr-N thin film with Th_3P_4 structure. *Appl. Surf. Sci.* **2009**, *255*, 6355–6358. [\[CrossRef\]](#)
106. Tham, A.T.; Roedel, C.; Lerch, M.; Wang, D.; Su, D.S.; Klein-Hoffmann, A.; Schloegl, R. A TEM study on ZrO_2 -rich phases in the quasibinary system $\text{ZrO}_2\text{-Zr}_3\text{N}_4$: Comparison between fast and slowly cooled samples. *Cryst. Res. Technol.* **2005**, *40*, 193–198. [\[CrossRef\]](#)

107. Walter, D.; Lerch, M.; Laqua, W. Thermal stability of the β'' phase in the $\text{ZrO}_2\text{-Zr}_3\text{N}_4$ system. *J. Therm. Anal.* **1997**, *48*, 709–716. [CrossRef]
108. Orlovskii, V.P.; Rudenko, N.V.; Ivanov-Emin, B.N. Thermal stability of zirconium tetrachloride ammines. *Zh. Neorg. Khim.* **1967**, *12*, 2305–2308.
109. Chhowalla, M.; Unalan, H.E. Thin films of hard cubic Zr_3N_4 stabilized by stress. *Nat. Mater.* **2005**, *4*, 317–322. [CrossRef]
110. Kroll, P. Assessment of the Hf-N, Zr-N and Ti-N phase diagrams at high pressures and temperatures: Balancing between MN and M_3N_4 (M = Hf, Zr, Ti). *J. Phys. Condens. Matter* **2004**, *16*, S1235–S1244. [CrossRef]
111. Kroll, P. Hafnium Nitride with Thorium Phosphide Structure: Physical Properties and an Assessment of the Hf-N, Zr-N, and Ti-N Phase Diagrams at High Pressures and Temperatures. *Phys. Rev. Lett.* **2003**, *90*. [CrossRef]
112. Binder, S.; Lengauer, W.; Ettmayer, P.; Bauer, J.; Debuigne, J.; Bohn, M. Phase equilibria in the systems Ti-C-N, Zr-C-N and Hf-C-N. *J. Alloys Compd.* **1995**, *217*, 128–136. [CrossRef]
113. Réjasse, F.; Rapaud, O.; Trolliard, G.; Masson, O.; Maître, A. Experimental investigation and thermodynamic evaluation of the C-Hf-O ternary system. *J. Am. Ceram. Soc.* **2017**, *100*, 3757–3770. [CrossRef]
114. Constant, K.; Kieffer, R.; Ettmayer, P. Pseudoternary hafnium oxide-hafnium mononitride-hafnium monocarbide system. *Monatsh. Chem.* **1975**, *106*, 973–981. [CrossRef]
115. Salamat, A.; Hector, A.L.; Kroll, P.; McMillan, P.F. Nitrogen-rich transition metal nitrides. *Coord. Chem. Rev.* **2013**, *257*, 2063–2072. [CrossRef]
116. Bredow, T.; Lerch, M. On the Anion Distribution in $\text{Zr}_7\text{O}_8\text{N}_4$. *Z. Anorg. Allg. Chem.* **2007**, *633*, 2598–2602. [CrossRef]
117. Locherer, T.; Dubrovinsky, L.; Fuess, H. Isothermal compression of nitrogen doped zirconia/zirconium oxonitride $\text{Zr}_7\text{O}_{11}\text{N}_2$ and equation of states. *Solid State Commun.* **2007**, *143*, 408–411. [CrossRef]
118. Lerch, M. Phase relationships in the $\text{ZrO}_2\text{-Zr}_3\text{N}_4$ system. *J. Mater. Sci. Lett.* **1998**, *17*, 441–443. [CrossRef]
119. Clarke, S.J.; Michie, C.W.; Rosseinsky, M.J. Structure of Zr_2ON_2 by Neutron Powder Diffraction: The Absence of Nitride–Oxide Ordering. *J. Solid State Chem.* **1999**, *146*, 399–405. [CrossRef]
120. Michie, C.W.; Claridge, J.B.; Clarke, S.J.; Rosseinsky, M.J. $\text{Zr}_4\text{O}_5\text{N}_2$ –Intergrowth of Fluorite and Bixbyite Anion Layers Formed by Coupled Site-Selective Anion and Vacancy Ordering. *Chem. Mater.* **2003**, *15*, 1547–1553. [CrossRef]
121. Razumovskiy, V.I.; Ghosh, G. A first-principles study of cementite (Fe_3C) and its alloyed counterparts: Structural properties, stability, and electronic structure. *Comput. Mater. Sci.* **2015**, *110*, 169–181. [CrossRef]
122. Zhang, Y.; Liu, B.; Wang, J.; Wang, J. Theoretical investigations of the effects of ordered carbon vacancies in ZrC_{1-x} on phase stability and thermo-mechanical properties. *Acta Mater.* **2016**, *111*, 232–241. [CrossRef]
123. Kim, C.; Pilania, G.; Ramprasad, R. Machine Learning Assisted Predictions of Intrinsic Dielectric Breakdown Strength of ABX_3 Perovskites. *J. Phys. Chem. C* **2016**, *120*, 14575–14580. [CrossRef]
124. Aigner, K.; Lengauer, W.; Rafaja, D.; Ettmayer, P. Lattice parameters and thermal expansion of $\text{Ti}(\text{C}_x\text{N}_{1-x})$, $\text{Zr}(\text{C}_x\text{N}_{1-x})$, $\text{Hf}(\text{C}_x\text{N}_{1-x})$ and TiN_{1-x} from 298 to 1473 K as investigated by high-temperature X-ray diffraction. *J. Alloys Compd.* **1994**, *215*, 121–126. [CrossRef]
125. Kornilov, A.N.; Chelovskaya, N.V.; Zhelankin, V.I.; Shveikin, G.P. Enthalpies of formation of hafnium carbides. *J. Chem. Thermodyn.* **1977**, *9*, 629–642. [CrossRef]
126. Brundiers, G.D. Herstellung, Aufbau und Eigenschaften von Hafniumverbindungen im System Hf-C-N-O. KFK-2161. Thesis/Dissertation, Karlsruhe Univ., Karlsruhe, Germany, 1975; p. 278. Available online: http://inis.iaea.org/search/search.aspx?orig_q=RN:07230513 (accessed on 23 August 2019).
127. Banus, M.D.; Reed, T.B.; Strauss, A.J. Electrical and Magnetic Properties of TiO and VO . *Phys. Rev. B* **1972**, *5*, 2775–2784. [CrossRef]
128. Adachi, G.-Y.; Imanaka, N.; Zhang, F. Rare earth carbides. In *Handbook on the Physics and Chemistry of Rare Earths*; Gschneidner, K.A., Jr., Eyring, L., Eds.; Elsevier: Amsterdam, The Netherlands, 1991; Volume 15, pp. 161–189. [CrossRef]
129. Butherus, A.D.; Eick, H.A. Preparation and some properties of the lanthanide oxide carbides, $\text{Ln}_4\text{O}_3\text{C}$. *J. Am. Chem. Soc.* **1968**, *90*, 1715–1718. [CrossRef]
130. Losego, M.D.; Mita, S.; Collazo, R.; Sitar, Z.; Maria, J.-P. Epitaxial growth of the metastable phase ytterbium monoxide on gallium nitride surfaces. *J. Cryst. Growth* **2008**, *310*, 51–56. [CrossRef]

131. Losego, M.D.; Maria, J.-P. Synthesis of polycrystalline ytterbium monoxide thin films by molecular beam deposition. *J. Vac. Sci. Technol. B* **2006**, *24*, 2111–2114. [CrossRef]
132. Leger, J.M.; Yacoubi, N.; Loriers, J. Synthesis of rare earth monoxides. *J. Solid State Chem.* **1981**, *36*, 261–270. [CrossRef]
133. Katz, J.J.; Morss, L.R.; Edelstein, N.M.; Fuger, J. *The Chemistry of the Actinide and Transactinide Elements*; Springer: Dordrecht, The Netherlands, 2007. [CrossRef]
134. Mazzoni, A.D.; Conconi, M.S. Study of carbonitriding reactions of zirconia. Synthesis of Zr(C,N,O) phases and β -type zirconium oxynitrides. *Ceram. Int.* **2004**, *30*, 23–29. [CrossRef]
135. Constant, K.; Kieffer, R.; Ettmayer, P. Pseudoternary zirconium monoxide-zirconium nitride-zirconium carbide system. *Monatsh. Chem.* **1975**, *106*, 823–832. [CrossRef]
136. Kornilov, A.N.; Chelovskaya, N.V.; Zhelankin, V.I. Heat of formation of zirconium carbides. *Zh. Fiz. Khim.* **1975**, *49*, 1341.
137. Pipon, Y.; Toulhoat, N.; Moncoffre, N.; Gutierrez, G.; Maitre, A.; Gendre, M. Influence of the Oxygen content on the thermal migration of Xenon in $\text{ZrC}_x\text{O}_{1-x}$. *J. Nucl. Mater.* **2013**, *440*, 546–552. [CrossRef]
138. Agte, C.; Alterthum, H. Systems of high-melting carbides; contributions to the problem of carbon fusion. *Z. Tech. Phys.* **1930**, *11*, 182–191.
139. Kato, H.; Copeland, M.I. *Report of Investigations*; U.S. Bureau of Mines: Washington, DC, USA, 1962.
140. Adams, R.P.; Beall, R.A. Preparation and Evaluation of Fused Hafnium Carbide. 1066–5552; U.S. Department of the Interior; Bureau of Mines, 1963; p. 17. Available online: <https://catalog.hathitrust.org/Record/005981077> (accessed on 23 August 2019).
141. Sara, R.V. The hafnium-carbon system. *Trans. Am. Inst. Min. Metall. Pet. Eng.* **1965**, *233*, 1683–1691.
142. Rudy, E.; Windisch, S. *Ternary Phase Equilibriums in Transition Metal-Boron-Carbon-Silicon Systems. Part 2 Vol. I*; AFML-TR-65-2; Aerojet-Gen. Corp.: Sacramento, CA, USA, 1965; p. 53.
143. Rudy, E.; Progulski, J. Pirani furnace for the precision determination of the melting temperatures of refractory metallic substances. *Planseeber. Pulvermetall.* **1967**, *15*, 13–45.
144. Deardorff, D.K.; Copeland, M.I.; Adams, R.P. Hafnium-carbon phase diagram. *US Bur. Mines Rep. Invest.* **1967**, *6983*, 16.
145. Cedillos-Barraza, O.; Manara, D.; Boboridis, K.; Watkins, T.; Grasso, S.; Jayaseelan, D.D.; Konings, R.J.M.; Reece, M.J.; Lee, W.E. Investigating the highest melting temperature materials: A laser melting study of the TaC-HfC system. *Sci. Rep.* **2016**, *6*, 37962. [CrossRef]
146. Kohn, W.; Sham, L.J. Self-Consistent Equations Including Exchange and Correlation Effects. *Phys. Rev.* **1965**, *140*, A1133–A1138. [CrossRef]
147. Perdew, J.P.; Burke, K.; Ernzerhof, M. Generalized gradient approximation made simple. *Phys. Rev. Lett.* **1996**, *77*, 3865–3868. [CrossRef]
148. Heyd, J.; Scuseria, G.E.; Ernzerhof, M. Hybrid functionals based on a screened Coulomb potential. *J. Chem. Phys.* **2003**, *118*, 8207. [CrossRef]
149. Baker, F.B.; Storms, E.K.; Holley, C.E., Jr. Enthalpy of formation of zirconium carbide. *J. Chem. Eng. Data* **1969**, *14*, 244–246. [CrossRef]
150. Yungman, V.S.; Glushko, V.P.; Medvedev, V.A.; Gurvich, L.V. *Thermal Constants of Substances*; Wiley: Hoboken, NJ, USA, 1974; p. 343.
151. Ettmayer, P.; Kieffer, R.; Hattinger, F. Determination of the melting point of metal nitrides under nitrogen pressure. *Metall* **1974**, *28*, 1151–1156.
152. Chase, M.W.J. *NIST-JANAF Thermochemical Tables*; American Inst. of Physics: University Park, MD, USA, 1998. Available online: <https://janaf.nist.gov/> (accessed on 23 August 2019). [CrossRef]
153. Meschel, S.V.; Kleppa, O.J. Thermochemistry of alloys of transition metals and lanthanide metals with some IIIA and IVA elements in the periodic table. *J. Alloys Compd.* **2001**, *321*, 183–200. [CrossRef]
154. Kornilov, A.N.; Ushakova, I.M.; Huber, E.J., Jr.; Holley, C.E., Jr. Enthalpy of formation of hafnium dioxide. *J. Chem. Thermodyn.* **1975**, *7*, 21–26. [CrossRef]
155. Kim, S.; Szlufarska, I.; Morgan, D. Ab initio study of point defect structures and energetics in ZrC. *J. Appl. Phys.* **2010**, *107*, 053521. [CrossRef]
156. Ushakov, S.V.; Navrotsky, A. Experimental approaches to the thermodynamics of ceramics above 1500 °C. *J. Am. Ceram. Soc.* **2012**, *95*, 1463–1482. [CrossRef]

157. Dworkin, A.S.; Bredig, M.A. Diffuse transition and melting in fluorite and antiferrotype type of compounds. Heat content of potassium sulfide from 298 to 1260 K. *J. Phys. Chem.* **1968**, *72*, 1277–1281. [[CrossRef](#)]
158. Hong, Q.-J.; Ushakov, S.V.; Kapush, D.; Benmore, C.J.; Weber, R.J.K.; van de Walle, A.; Navrotsky, A. Combined computational and experimental investigation of high temperature thermodynamics and structure of cubic ZrO_2 and HfO_2 . *Sci. Rep.* **2018**, *8*, 14962. [[CrossRef](#)]
159. Schroeder, W.; Pottlacher, G. Estimation of critical data and phase diagrams of pure molten metals. *High Temp. High Press.* **2014**, *43*, 201–215.
160. McGrath, J.R. *Exploding Wire Research 1774-1963. NRL Memorandum Report 1698*; AD0633623. US Naval Research Laboratory: Washington, DC, USA, 1966. Available online: <http://www.dtic.mil/docs/citations/AD0633623> (accessed on 23 August 2019).
161. Onufriev, S.V.; Savvatimskiy, A.I. Measuring the Specific Heat of Conducting Substances in Conditions of Microsecond Heating with a Current Pulse. *High Temp.* **2018**, *56*, 678–684. [[CrossRef](#)]
162. Knyazkov, A.M.; Kurbakov, S.D.; Savvatimskiy, A.I.; Sheindlin, M.A.; Yanchuk, V.I. Melting of carbides by electrical pulse heating. *High Temp. High Press.* **2011**, *40*, 349–358.
163. Hong, Q.-J.; van de Walle, A. Solid-liquid coexistence in small systems: A statistical method to calculate melting temperatures. *J. Chem. Phys.* **2013**, *139*, 094114. [[CrossRef](#)]
164. Van de Walle, A.; Ceder, G. The effect of lattice vibrations on substitutional alloy thermodynamics. *Rev. Mod. Phys.* **2002**, *74*, 11–45. [[CrossRef](#)]



© 2019 by the authors. Licensee MDPI, Basel, Switzerland. This article is an open access article distributed under the terms and conditions of the Creative Commons Attribution (CC BY) license (<http://creativecommons.org/licenses/by/4.0/>).